IEEE Access
Multidisciplinary ⋮ Rapid Review ⋮ Open Access Journal

Received 20 March 2023, accepted 5 April 2023, date of publication 11 April 2023, date of current version 14 April 2023.

Digital Object Identifier 10.1109/ACCESS.2023.3265999

TOPICAL REVIEW

A Review of Dynamic Vehicular Motion Simulators: Systems and Algorithms

MOHAMMADALI GHAFARIAN, (Member, IEEE), MATTHEW WATSON, NAVID MOHAJER, DARIUS NAHAVANDI, (Member, IEEE), PARHAM MOHSENZADEH KEBRIA, (Member, IEEE), AND SHADY MOHAMED

Institute for Intelligent Systems Research and Innovation (IISRI), Deakin University, Waurn Ponds, VIC 3216, Australia

Corresponding author: Mohammadali Ghafarian (m.ghafarian@deakin.edu.au)

ABSTRACT Vehicular motion simulators have evolved to become an important contributor to major industries, including defense, aerospace, and vehicle manufacturing. During the past few decades, many efforts have been made towards developing robust, adaptive motion simulators with the highest level of fidelity and realism. Thus, it is important to recollect, in order to evaluate the current state of complex robotic systems, encouraging careful planning of further improvements in the future. This article focuses on the current motion simulators' structural designs and working principles alongside the currently developed motion control algorithms to achieve the highest fidelity. Furthermore, within the era of industry 4.0 and the fast-paced merging of technologies into key industries, some suggestions are made for future works which it is believed are worth investigating to provide robustness and adaptivity to the control of simulation systems, improving their fidelity and realism alongside reducing motion sickness experienced by the simulator operator.

INDEX TERMS Driver-in-the-loop simulation, simulation fidelity, simulation sickness, vehicular motion simulator.

I. INTRODUCTION

Vehicular simulators are playing an expanding role in different applications [1] including vehicle dynamics (tire development, driver training, control system design, and tuning of the chassis), autonomous vehicle (AV), advanced driver assistance systems (ADAS), vehicle development, V2X studies and more. The high-bandwidth dynamic simulator establishes new standards as well. Thus, the simulation of extremely dynamic evasive maneuvers, complete braking, and strong acceleration is possible. The industries and the regulatory bodies feel that this has resulted in a cost-effective means of manufacturing, improving the safety records, and enhancing the current state of vehicular technologies. Vehicle manufacturers invest significant capital on testing and performance assessments for every new design of a vehicle, such as the axles, chassis, suspension, engine, gear-shifting modes, steering, and brake controls, etc. In addition to being expensive, testing with real prototype vehicles takes significant time and can pose risks for the test drivers. By utilizing cutting-edge motion platform-based driving simulators, which offer a lifelike virtual experience for vehicle prototyping and virtual vehicle testing, these drawbacks can be significantly reduced or completely eliminated. Moreover, as autonomous driving becomes more prevalent and the advancement of driving assistance systems, vehicle manufacturers are putting more emphasis on high-performance driving simulation to test new features and improve driving comfort before production [2]. For instance, ADAS market size is estimated to be worth USD 29.74 billion in 2022 and is forecast to be a re-adjusted size of USD 57.76 billion by 2028 [3]. This is compounded by the increasing government legislations, mandating new vehicles have basic ADAS features by 2030. Physical prototypes can be delayed until much closer to final production since driving simulators make testing possible far earlier in the vehicle development process. Thus, simulators are an essential component of the vehicle development process. The phases of vehicle design are naturally connected by the results

The associate editor coordinating the review of this manuscript and approving it for publication was Shihong Ding.

from simulator tests. From 2019 to 2021, the GMC's 1000-hp Hummer EV went from being a concept car to a product launch. To re-establish the Hummer brand as the company's design leader, 17 new features were added during the process. This quick development is entirely attributable to the motion simulator that was used in the design process, where the new EV was fully engineered in a virtual environment before the first actual prototypes ever left a production line. With this project delivered, the high-tech simulator used for Hummer EV, is now set to be utilized for another futuristic and ambitious project. The Lunar Mobility Vehicle (LMV) is a joint Lockheed Martin and General Motors project to develop the next generation of lunar and martian rovers. Potentially expensive flaws can be found before they appear in a real, and possibly very remote world by having the ability to accurately simulate a lunar environment, where vehicle properties can be adjusted and tested in real-time here on Earth. Engineers can modify a vehicle's top speed, turning angle, torque, suspension travel, and other driving dynamics using high-fidelity vehicular simulators. These parameters must be tuned to one-sixth of Earth's gravity acting on a vehicle as it transits the highly abrasive, rocky, and disorienting lunar surface. Once vehicle specifications are confirmed, the simulator will eventually be utilized to help give astronauts a sense of what driving on the moon is like.

The most crucial element of a simulation is immersion [4]. The driver must experience driving in a real vehicle and in a realistic environment. The way they react to the virtual environment around them and the virtual vehicle they are driving must be a replica of the real-life scenario. Every element needs to accurately replicate the feel and response of the driving experience. The value of the resulting data and feedback increases as the gap between the simulated and real worlds is reduced.

Advances in technology are resulting in a steady improvement in the fidelity and the effectiveness of vehicular simulators [5]. In modern simulators the motion generation system is one of the major subsystems employed to create realistic virtual worlds that draw the humans in to the experience. Recent hardware developments have improved the fidelity of these motion systems significantly, with increased processor speed complementing projector systems with greater resolution. Because of things like the extent of the accessible workspace and the intrinsic resistance that results from the motion actuators' operation, driving simulators are constrained environments within the simulated environment. A control block that is a component of the software running any motion platform must manage the position of the cabin by giving the driver a realistic sense of acceleration and deceleration. For a high-fidelity driving simulator, it is necessary that the human does not find any differences between the experience of driving in the simulator's virtual environment versus the experience encountered on the road in a real vehicle. To accomplish that, the vehicle model must be as accurate as possible and the feedback, that renders information about the current simulated situation in real-time, must be well reproduced to ensure the correct interaction between the user and the simulation. Because a ground-based motion simulator system cannot duplicate the motions of an actual vehicle it becomes necessary to determine the best way to utilize the full spectrum of motion within the constraints of its capabilities. This, in turn, requires a determination of how motion inputs are detected and interpreted by human operators. The motion-base drive software algorithms are intended to maximize the motion cueing effect while restricting the physical motion: the simulated environment may use only the displacement, velocity, and acceleration capacity of the motion system hardware.

It is very complex, almost impossible, to reproduce exactly the large-scale motion of a vehicle in the limited workspace of a motion platform. A proper motion strategy must be set to deceive the human perception of the sensed acceleration to reproduce the experience of those large motions with only abbreviated movements. As a result, Motion Cueing Algorithm (MCA) strategies have been developed [6], [7], [8], [9], [10], [11], [12], [13], [14], [15], [16], [17], [18], [19], [20], [21], [22], [23], [24], [25], [26], [27], [28], [29], [30], [31], [32], [33], [34], [35] to define the motion of the platform and deceive the human vestibular perception. However, these strategies could generate the perception of false cues due to imperfections and consequently do not match the visual stimulation [36]. These false cues generate fatigue and discomfort in the operator. Hence, false cues must be at least reduced, if not eliminated, to increase the simulator's fidelity.

The computer software that commands the motion system needs further refinement. The lack of realistic motion cues during various conditions and maneuvers is still a constant problem experienced by the drivers, pilots, and helmsmen. In some instances, they resort to effectively turning off the motion system to avoid improper cues. Motion and simulator sickness [37], [38], [39], [40] can arise in some participants through a conflict that arises between different sensory systems, i.e. the signals from visual, vestibular, and non-vestibular proprioceptors differ from one another and inevitably differ with expectations based on previous experience. This conflict between present sensory information, and that retained from the immediate past, elicits sickness. Moreover, it has been discovered that regardless of the type of vehicle simulated, transport delay effects [41], [42] are similar. They mainly fall under the control degradation and simulator sickness categories. Both these effects have the potential to adversely affect research data collected in a simulator as well as training effectiveness. The asynchronous architecture of the software is found to be a significant cause of transport delay. Furthermore, the hardware-related transport delay should be investigated in order to identify the ideal configuration for a high-performance, full-scale dynamic vehicular simulator [43]. The asynchronism between vision and motion systems expresses a latency gap which is regarded as the key latency contributing to simulator sickness and should be

minimized as much as possible. As an emphasis, the response time to input and feedback must have the lowest possible latency. The delivery of vestibular, auditory, haptic, and visual cues to the driver's senses must occur with the least amount of delay possible. Another considerable requirement is that the rendered motion must be synchronized with the visual stimulation to reproduce a realistic driving sensation. The overall system latency has to be minimal, e.g. below the required 180 ms for vehicular simulators [44], otherwise, the driver will feel fatigued and uncomfortable after their experience in the simulated environment. This latency can be reduced using compensation algorithms. These compensators, which are essentially filters, are developed to provide enough phase lead at frequencies crucial to driver control to compensate for inherent system delays. In simulation tests, three compensation methods (lead/lag, three-velocity-term predictive filter, and four-velocity-term predictive filter) appear to handle improvements. Although minimizing or eliminating transport delays will not stop participants from feeling discomfort, they could be highly helpful in enhancing the realism of a particular simulator.

In technical terms, motions simulators are based on the utilization of an electromechanical system integrated with multiple actuators and sensors [45], [46], [47], [48], [49]. These mechanisms are often capable of generating different kinds of translational and rotational motions in different axes and are categorized into serial, parallel, and hybrid structural principles. Each principle provides different pros and cons. Numerous benefits come with using a serial robot as a motion simulator [50], [51], [52], including high dexterity, sustained centrifugal accelerations, a large motion envelope, and the ability to position subjects in extreme orientations (e.g. upside-down) [53]. On the other hand, Stewart platforms with a hexapod motion system [24], [39], [54], [55], [56], [57], [58], [59], [60], [61], [62], [63] are advantageous for motion simulation because of their position accuracy, dynamic efficiency, and payload to weight ratio.

Different aspects of these kinds of complex motion simulators have been utilized in over a dozen countries, and researched over the past two decades. Now seems an appropriate time to step back and look at where we are and where we intend to go from here. Thus, in the present work, a comprehensive review of the past and current state-of-the-art dynamic vehicular simulators and particular aspects of vehicular systems and simulation algorithms is investigated as a guide for future improvements and applications. The goal of a vehicular simulator is to create a motion simulation with the highest level of fidelity and realism. Figure 1 shows how different systems including hardware and software are integrated and work collaboratively to achieve that goal. The vehicle operator and vehicle model are at the center of the process. Operator input is used to calculate the vehicle dynamics by the vehicle model, which will be used by the feedback systems including steering wheel, gear selector, foot pedals, active seats, seat belts, actuated dashboard and heel rest to

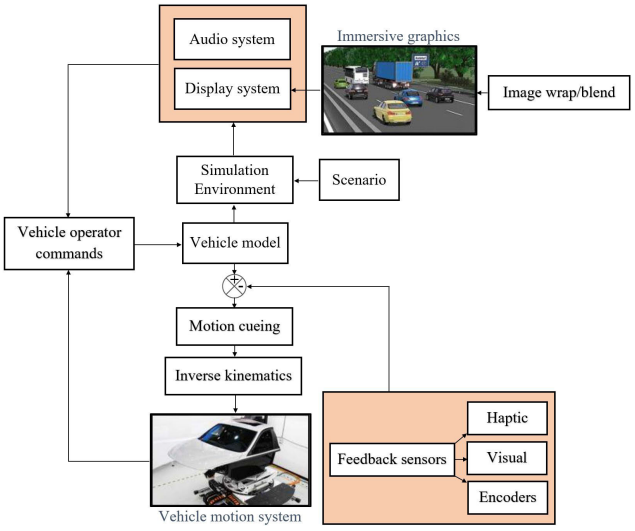

FIGURE 1. Schematic diagram of a driving simulator.

give the driver the necessary cues. These cues are signaled by the human vestibular and proprioceptive sensory systems and can be reproduced in dynamic simulators by controlling their mechanical actuators within certain limits in terms of displacement, velocity, and acceleration. The scenario control outputs, visual and auditory cues using the created simulated environment, as well as the vehicle dynamics. Moreover, the generated scenario is projected onto a curved screen using multiple projectors to create an immersive experience: one of actually operating a vehicle. Finally, the motion cueing algorithm will use the vehicle response to calculate how to move the motion system while accounting for the system's kinematics, be converted into actuator command by the machine's kinematics, and then be generated by the motion system delivering cues to the human operator.

This paper is organized as follows. Section II introduces the current state-of-the-art vehicular simulators in research and industry and categorizes them based on their robotic working principle, degrees of freedom (DoF), and the manufacturing country. Section III explains the motion cueing algorithms that have been developed and utilized to date for achieving a vehicular simulator with high fidelity. Section IV discusses the optimization methods that have been utilized, or have the potential to be utilized, for automation of the tuning parameters of motion cueing algorithms to find the optimal parameters for each system, and reduce the computation time and power. Finally, Section V concludes the work and states the prospects for vehicular simulators.

II. MOTION SIMULATORS

The available motion simulators which have been used for commercial and/or research purposes are reviewed in this section comprehensively. Table 1 outlines these complex advanced robotic systems based on their company, name, working principle, degrees of freedom, and their location.

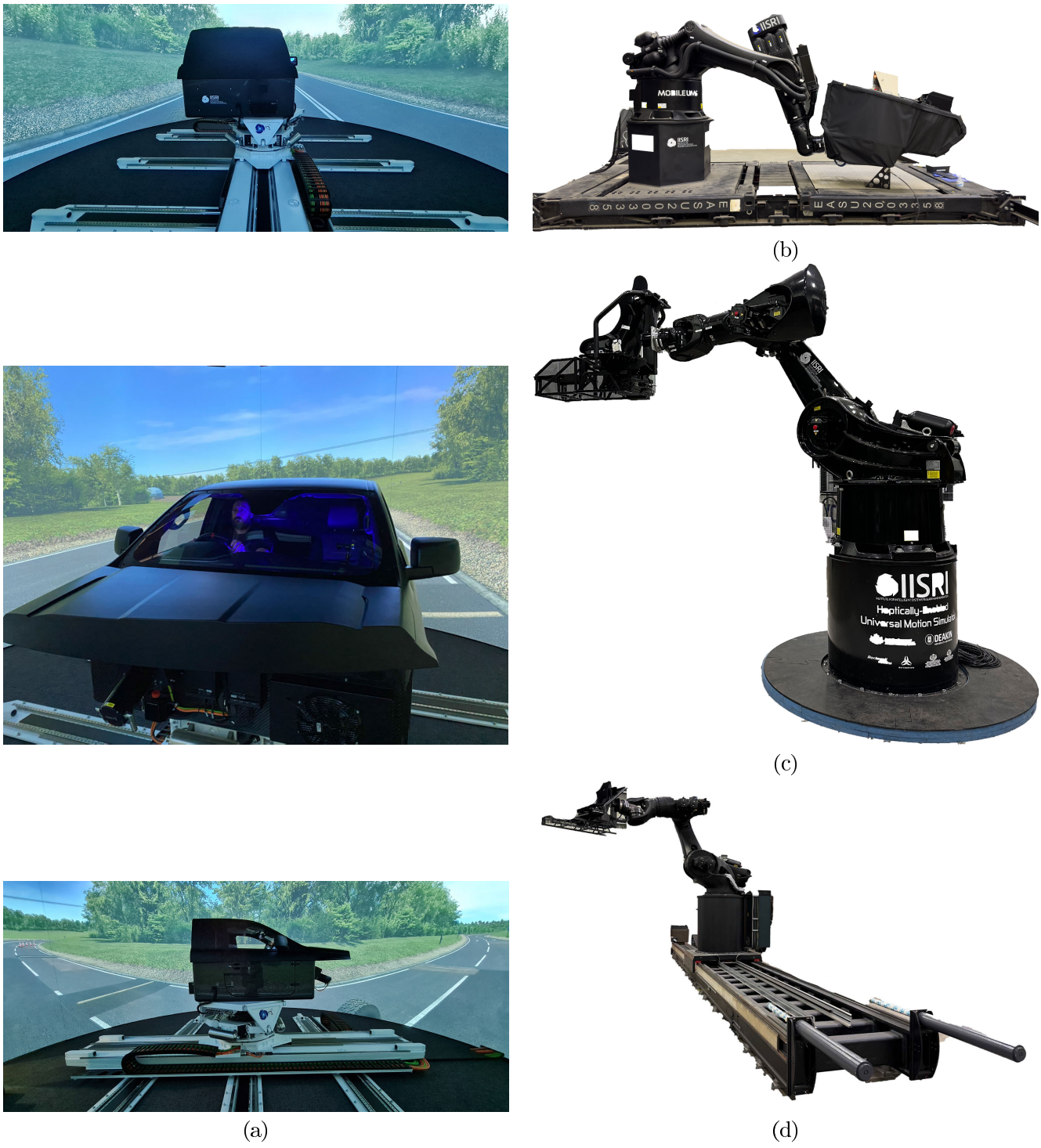

FIGURE 2. IISRI motion simulators: (a) Genesis, (b) Mobile, (c) Core, (d) Infinity.

A. IISRI MOTION SIMULATOR

Universal Motion Simulator (UMS) [64], [65], [66] was developed by the Institute for Intelligent Systems Research and Innovation (IISRI) at Deakin University in Australia (Figure 2(b-d)). Presently, IISRI is home to several types of motion simulators, i.e. UMS Core, Mobile UMS and UMS Infinity. The UMS platform is based on a KUKA commercial off-the-shelf robot. Through the use of haptic vehicle controls, an immersive high-resolution head-mounted display capable of 3D visualization, head-tracking ability, and a complete set-up of 36 motion capture cameras and tracking system, the UMS family offers total immersion in

the simulation world. The UMS can also perform physical monitoring, such as electrocardiogram (EEG) and heart rate monitoring.

The latest addition to the IISRI motion simulators family is the next generation of realistic advanced motion simulator with 360-degrees platform view, which has the Ansible Delta S3 simulator at its heart (Figure 2(a)). The Delta S3 delivers accelerations up to 2G, velocities up to 5m/s and 200deg/s, and a class-leading frequency response of about 40Hz for each axis. The 360-degrees graphics is visualized using 12 Norxe P1+ WQXGA projectors with 2560 × 1600 resolution, 3000 RGB ANSI lumens and 16:10 aspect ratio. Furthermore, the projectors have a 2-DoF lens shift feature. The simulator is capable of full 360° dynamic yaw rotations, and a set of engineered linear rails - 4m in length - enables sustained, independent sway and surge motions for a more immersive and representative experience for maneuvers such as aggressive lane changing, autonomous parking and anything in between. The mechanism that bears the cabin offers an additional 3-DoF to the vehicle motion profile: heave, pitch, and roll. Importantly, this design enables the dynamic exercise of a vehicle cabin up to 500 kg in all 6 DoF, the maximum possible for fully defining the motion of a 3D body, at any point in a spatial space. Moreover, the cabin is equipped with a 2-DoF Seat Vibration Loading System (SVLS) which provides vehicle physics-derived high frequency motions directly to the driver's seat. This system allows the driver to experience the slightest road details transferred to the seat. The SLVS system has 12mm motion in each axis with the frequency range up to 200Hz. This simulator is an advanced research and innovation platform to be utilized for both driver-based and driver-less (autonomous) mobility technologies, plus research in human-centered advanced mobility factors.

Many channels of data are available in Genesis to record from. Some examples of the Genesis simulator's results are shown in Figures 3 and 4. The data transmission rate was set at the frequency of 100Hz, however it can be maximized to 1kHz if needed. The results are as expected and shown within the motion platform system to replicate the expected behavior defined by the Physics model.

B. ANSIBLE MOTION SIMULATORS

Ansible Motion's Delta DIL simulator [67], [68], [69], [70] is a sophisticated, high-performance, dynamic driving simulator. It aims to satisfy the increasing demand for human-centered, high-fidelity, high-dynamic vehicle simulations in both road and racetrack applications. Designed and manufactured in-house in Norfolk, UK, it has a scalable architecture meaning it can be built and delivered in various sizes, making it ideal for a wide range of automotive product development use cases such as expert driver assessments, chassis dynamics, powertrain driveability, V2X research, ADAS and active safety function calibration, and Human-Machine Interface (HMI) design evaluations. Mindful of the flexibility that has made such driving simulators popular with development engineers, the Delta offers an open software and hardware architecture that facilitates the use of essentially any option for real-time vehicle modelling, scenario simulation, graphical rendering, or supplemental cueing, whether they are sourced from Ansible Motion themselves or a third party.

C. FORD's DRIVING SIMULATORS

The Ford Performance Technical Center in Concord, North Carolina, opened in 2014. The facility serves as a Center of Excellence for Ford NASCAR and IMSA race teams to test theories and refine driving skills through the use of full-motion platform simulators [62], [71]. At the Center, various bucks can be installed on the motion platforms. Whether it's a Ford GT endurance racer or a NASCAR Sprint Cup car, each buck is built to replicate the interior of different automobiles as accurately as possible. To generate a virtual model of each vehicle, engineers feed data from a variety of sources, including engine dynamometers and kinematics and compliance devices that measure suspension motion. This simulator is a great tool since the model precisely recreates all of the measurements of a particular car. This buck and the virtual model is then run on a simulated road surface - such as a testing facility or a given road. As the Ford team stated, running the simulator is undoubtedly an expensive endeavor, but it is considerably less expensive than sending cars and personnel to tracks around the world. On a virtual replica of the infamous Nürburgring track in Germany, the Ford team tested the Mustang GT500. Furthermore, they virtually tested five different aerodynamic GT500 kits, which was a much faster and less expensive process than manufacturing and swapping out five separate sets of wings, splitters, and other aerodynamic components. In conclusion, evidence shows use of high-fidelity simulation at this stage has saved time and money in manufacturing a new car.

D. BEC SIMULATOR

BEC, a German company, incorporates KUKA industrial robots into cutting-edge simulators for virtual reality research, dynamic pilot training, and driving simulations. The BEC motion simulator originally has 6-DoF, however, this can be customized by adding more axes of motion (e.g. a linear axis or curved rail on the pod). It can also operate with cockpits customized for each customer. Thus, the motion range can be expanded to 8-DoF. The simulator pod's modular architecture allowed for the simple swap of instrument modules and the ability to simulate various aircraft or helicopters.

E. MAX PLANCK INSTITUTE (CYBERNEUM)

The Cyberneum is part of the Max Planck Institute, located at Tübingen, Germany. This facility is home to three kinds of motion simulators, i.e. CableRobot, CyberMotion, and CyberPod. The CableRobot simulator employs a parallel kinematics architecture, where winch-driven cables are used in place of the rigid linkages found in other simulators. The

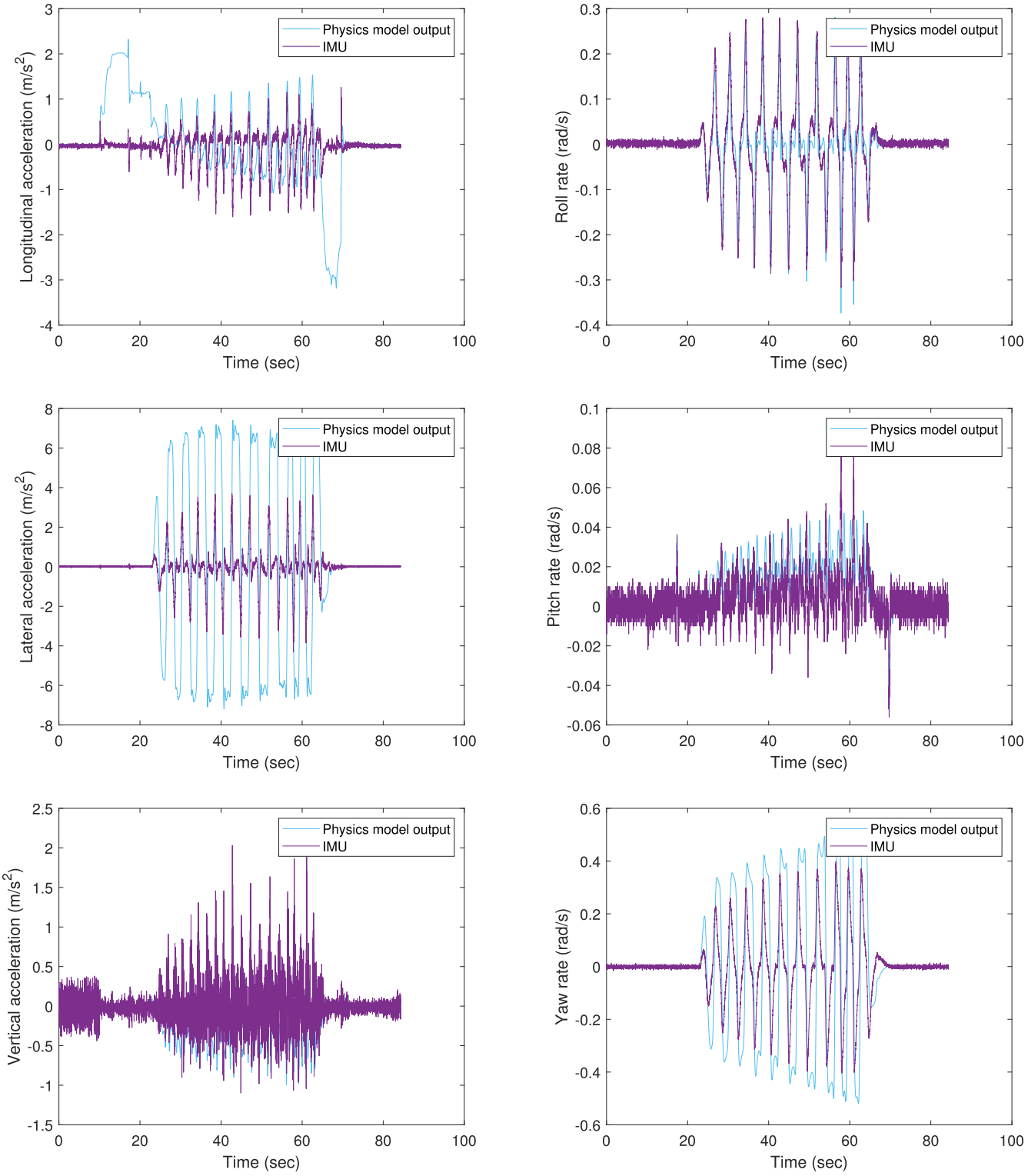

FIGURE 3. Comparison of the accelerations and velocities generated by physics model and IMU mounted on the platform of the motion system.

power-to-weight ratio of the CableRobot is approximately 2.6 kW/kg, and it can be operated at a maximum acceleration of 5m/s^2 in a workspace of 5 × 6×4 m^3, and maximum roll, pitch, and yaw angles of ±40°, ±40°, ±5° respectively.

The CyberMotion Simulator [53], [72] is a six-axis industrial robot arm that is extended by an L-shaped cabin axis. By moving the cabin's attachment point from behind the seat to under the seat, or any other intermediate position, the

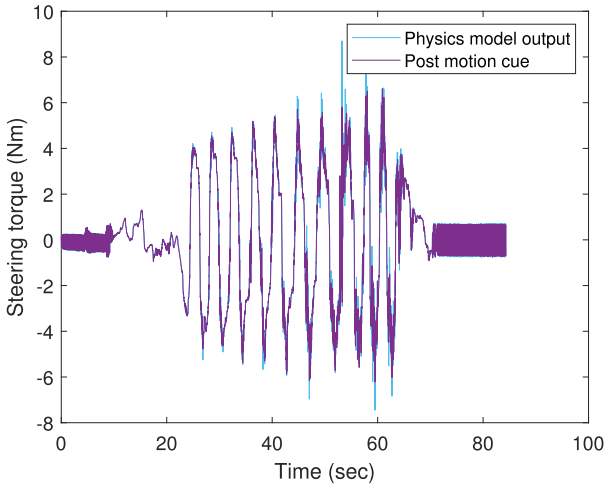

FIGURE 4. Comparison of the steering torque generated by physics model and post motion cue signal from the electric steering torque motor.

seventh axis enables the cabin's orientation with respect to the robot arm to be altered. Moreover, a ten-meter linear axis has been fitted to the CyberMotion unit. A large workspace is provided by the resulting 8-DoF. It is possible to produce a variety of extreme motions and positions, including upside-down motions, sustained centrifugal motions, large lateral/longitudinal motions, and infinite head-centered rotation. A stereo projection system (eyevis GmbH) with a field-of-view (FOV) of 140° H × 70° V and a resolution of 1920 × 1200 on each projector is installed in the cabin. With projection filters and glasses (Infitec), high-fidelity 3D visualization is possible. The centerpiece of the MPI CyberPod is a 6-DoF Bosch Rexroth eMotion-1500 hexapod Stewart platform. An Aluminum platform measuring 2.5 by 2.2 meters is mounted on the motion base. The platform has a detachable projection screen for visualizations that is placed 1.1 meters from the user and has a FOV of roughly 95° by 53°. Instead of the projection screen, the platform can also be utilized in combination with head-mounted display systems and optical tracking systems to measure head poses and the position of the simulator in the room. Auditory stimulation can be supplied using either noise-canceling headphones or a surround sound system.

F. DLR ROBOTIC MOTION SIMULATOR

The DLR Robotic Motion Simulator [50], [51], [52] is made by the Institute of Robotics and Mechatronics, located within the German Aerospace Center. It is an interactive motion simulator based on an industrial robot (Robocoaster (KUKA KR500-2)). Additional to the six axes of the robot, a seventh linear axis (KUKA KL3000 linear axis) increases the span of motion (to 10 m lateral) and allows redundancy for movements. At the tool center point, a simulator cell is mounted which consists of exchangeable instruments, input devices, two projectors and safety equipment. Moreover, utilizing two slip rings, one in axis 1 (the first rotational axis in yaw direction) and another in axis 6 (last axis before the simulator cell) it is possible to generate unrestricted rotation around the yaw and roll axis. This can be used to display yaw and roll motions of cars or airplanes directly without scaling down the resulting angular velocities.

G. SimAero

SimAero is a provider of flight simulator training and headquartered in Paris, France. The working principle of the SimAero is based on a 6-DoF Stewart mechanism. The company's flight simulators and training solutions cover a range of aircraft types including Airbus A320, A330, A340; Boeing 737, B757, B767; ATR 500, 600; ERJ 145; Beechcraft 1900; Dash 8; MD80/82; Fokker 100, Fokker F28.

H. AXIS SIMULATOR

AXIS Flight Training Systems GmbH was founded in 2004 in Austria. It manufactures flight simulators for different types and configurations of aircraft, including business jets, turboprop commuters, and passenger jetliners. These pilot training simulators are developed based on a Stewart mechanism.

I. DELFT VEHICLE SIMULATOR

These simulators are based on a Stewart platform and built by Delft University researchers. Delft Advanced Vehicle Simulator (DAVSi) [54] is a motion platform which can have motions in three translational directions (surge, sway and heave) and three rotational directions (roll, pitch and yaw). Therefore, it can imitate the motion of a freely suspended body. SIMONA Research Simulator (SRS) [55] is another 6-DoF simulator developed by the Delft University of Technology. This system is mainly a flight simulator tool that serves as a testbed for new technologies and as a tool for Human-Machine Interaction (HMI) research. The third Delft's vehicle simulator is MOTORIST, a motion-based riding simulator [56] that uses a mock-up Piaggio Beverly 350 cc motorcycle which is installed on a 6-DoF Stewart motion platform. The throttle handle and two brake levers are used by the rider to control the motorcycle. Independent of one another, the front and rear brake levers operate. Furthermore, to enhance the fidelity of the motorcycle-riding experience, the rider is encouraged to wear a helmet and a protective jacket. A helmet-mounted monitor is also used to generate the rider's virtual visual environment.

J. CRUDEN SIMULATOR

Cruden B.V. is a Dutch motion-based racing simulator company that manufactures static and motion-based driving and fast craft simulators which may be developed to suit a broad range of budgets and specifications. Its simulators meet the testing needs of automotive OEMs and their technology suppliers, race teams and motorsport engineering companies, the defense industry, including naval training organizations, and universities and research institutes.

For instance, the Cruden motorcycle simulator [57], [58] consists of a mock-up Ducati 848 EVO motorcycle installed

on a 6-DoF Stewart motion platform and a head mounted display (HMD) for the visualization of a surrounding virtual environment.

K. RENAULT DRIVING SIMULATOR

Renault 8 axis vehicle simulator [24], [59], [73], [74] was built in 2004 and updated in 2012. The system is a 6-DoF Stewart mechanism sitting on a 2-DoF XY linear platform, and is located at the Renault's virtual reality and immersive simulation center, Guyancourt, France. The simulation scenario is shown on a cylindrical screen with a FOV of 210°, horizontally. Moreover, a manual transmission, steering force feedback, and a sound system that reproduces engine and environmental noises are all included in the cockpit.

L. AVSimulation

AVSimulation designs, sells and maintains a wide range of automotive simulation software and simulators. The simulations are available on different operating systems and, are used in hardware-in-the-loop (HIL), software-in-the-loop (SIL), Model-in-the-loop (MIL) test benches, massive simulation in the cloud or located on-site. The Renault Automobile company is stakeholder of the AVSimulation and uses their simulator at the Renault Optimization Autonomous Driving Simulator (ROADS) facility, in Guyancourt, France.

M. VI-GRADE

VI-grade [63] is a developer of real-time simulation and driving simulator solutions across the transportation industry and, headquartered in Darmstadt, Germany. The developed driving simulators by this company, which range from static deskside solutions to full-scale driver-in-the-loop dynamic simulators, enable research facilities, universities, OEMs, suppliers, and motorsport teams to lessen their reliance on purpose-built physical prototypes and, through avoiding the need to construct and evaluate these, accelerate innovation.

N. TOYOTA DRIVING SIMULATOR

In order to help with the development and verification of traffic accidents and the reduction of active safety technology, Toyota Motor Corporation (TMC) [39] has established a driving simulator that analyzes the driving characteristics of typical drivers effectively. Furthermore, this facility enables vehicle researchers and engineers to carry out driving experiments that would be too risky and unsafe or necessitate particular driving circumstances to be present in the real world. A crucial component of this driving simulator is a real car mounted on a platform inside a 7.1-meter-diameter dome with a large 360-degree concave video screen covering the dome's ceiling. The dome can move 35 meters in longitudinal and 20 meters in lateral directions.

O. NADS-1 SIMULATOR

The National Advanced Driving Simulator Center houses a high-fidelity simulator, NADS-1, based at the College of Engineering, University of Iowa, USA. Vibrations emulating road sensation are produced by four hydraulic actuators connected to the cab. A yaw ring supporting the 7.3-meter dome provides for a 330° rotation of the dome around its vertical axis. The XY assembly moves inside a 19.5 × 19.5 meters bay to generate lateral and longitudinal accelerations. The NADS-1 motion system can give the driver precise motion cues that enable the driver to feel steering, braking, and acceleration, as well as experience extreme maneuvers typically associated with dangerous driving scenarios. The NADS-1 system displays a virtual environment with high-fidelity graphics, using sixteen high-definition LED projectors for seamless imagery on the interior walls of the dome resulting in a 360 degree horizontal and 40 degree vertical field of view.

P. aVDS SIMULATOR

The advanced Vehicle Driving Simulator (aVDS) is a driving simulator which utilizes linear actuators to deliver 6-DoF dynamic performance, providing low latency and high-frequency response. The motion platform can be quickly configured to take a variety of payloads up to 500kg, facilitating the installation of real vehicle cabins to suit particular simulation requirements.

Q. KRAKEN DISORIENTATION SIMULATOR

The KRAKEN spatial disorientation training simulator is the U.S. Navy's $19 million beast, which is a dynamic, cutting-edge motion system with multipurpose capabilities. It mimics the extreme maneuvers and physiological pressures endured by drivers and passengers of different kinds of vessels and vehicles, including the U.S. Navy's aviation operations involving flight operations with aircraft-carriers at sea. This simulator can be used for innovative human factors research as well as flight training for all sorts of naval aviation aircraft. For instance, areas of application in naval aviation include, but are not limited to, spatial disorientation (SD), accident recreation, upset recovery scenarios, loss of control in flight (LOCI), human factors research, and many more. Moreover, this simulator can sustain G acceleration up to ±3G.

R. NOVA VR

Nova VR is made by Eight360, a startup company in Wellington, New Zealand. The company's motion simulator can turn 180-degrees in any direction in only one second, combining visual, audio, and physical elements to allow users to experience immersive content as realistic as possible.

S. DESMORI MOTORCYCLE SIMULATOR

The DESMORI dynamic motorcycle riding simulator is built by Würzburg Institute for Traffic Sciences, a company based in Veitshöchheim, Germany, and it is equipped with a BMW F800S installed on a hydraulic Stewart platform with 6-DoF motion. The handlebar, gear selector, clutch, brake pedal/lever, and other motorcycle parts can all be operated by the rider. A sequential six-speed gearbox is used by the installed manual gearshift to allow for faster shifts. A steering

TABLE 1. Summary table of the reviewed dynamic vehicular simulators.

Company/Organization/Institute	Robotic simulator	Principle	DoF	Country
Flight/Car simulator				
IISRI	Genesis	Hybrid	8	Australia
https://youtube.com/playlist?list=PL07609E82877272CD				
IISRI	Core	Serial	6	Australia
https://youtu.be/Y-skv7GtXFc				
IISRI	Mobile	Serial	6	Australia
https://youtu.be/8ikxLa6W8CA				
IISRI	Infinity	Serial	7	Australia
Ansible Motion	Delta	Hybrid	6	United Kingdom
Ford	Virttex	Parallel	6	United States
Ford	Delta	Hybrid	6	United States
Ford	DiM250	Parallel	9	United States
https://youtu.be/6uH23IbgQFU				
BEC	BEC MS-506	Serial	6	Germany
BEC	BEC MS-506-H	Serial	7	Germany
BEC	BEC MS-507	Serial	8	Germany
BEC	BEC MS-506-L	Serial	7	Germany
BEC	BEC MS-1006	Serial	6	Germany
BEC	BEC MS-506-Mobil	Serial	6	Germany
BEC	Gimbal Simulator	Serial	3	Germany
https://youtu.be/wPj5cjoI3EI				
Cyberneum	CableRobot	Parallel	6	Germany
https://youtu.be/ihoEf5YgKiE				
Cyberneum	CyberMotion	Serial	8	Germany
https://youtu.be/ThkymYRP1g8				
Cyberneum	CyberPod	Parallel	6	Germany
DLR	DLR Simulator	Serial	7	Germany
https://youtu.be/QCGcWOwV8Qs				
DLR [75], [76]	dynSim	Parallel	6	Germany
https://youtu.be/RWZy3S7efIY				
SimAero	SimAero simulator	Parallel	6	France
AXIS	AXIS simulator	Parallel	6	Austria
Delft University	DAVSi	Parallel	6	Netherlands
https://youtu.be/hd7KIOI4-wA				
Delft University	SRS	Parallel	6	Netherlands
Curtin-Monash Accident Research Centre	C-MARC	Parallel	6	Australia
https://youtu.be/b7vEmczAM6I				
Cruden	AS1,AS2,AS3	Parallel	6	Netherlands
https://youtu.be/vyhW0cXmdfA				
General Motors	GM Simulator	Parallel	6	United States
General Motors	Delta	Hybrid	6	United States
Renault	ULTIMATE	Hybrid	8	France
AVSimulation	SimPULSE	Hybrid	8	France
VI-GRADE	DiM250	Parallel	9	Germany
https://cdn.vi-grade.com/ovh95/vigrade2020.com/dynatc/desktopvideos-1297-3554/dim-in-action-release-2020-1.mp4?210713122726				
VI-GRADE	DiM400	Parallel	9	Germany
https://cdn.vi-grade.com/ovh95/vigrade2020.com/dynatc/desktopvideos-1283-c608/monza_mark_def_rev1-1024.mp4?210629120345				
Polytechnic University of Milan	DiM400	Parallel	9	Italy
Toyota Motor	Toyota Driving Simulator	Hybrid	8	Japan
Honda Motor	Delta	Hybrid	6	Japan
Honda R&D Europe	DiM250	Parallel	9	Germany
Mazda Motor [77]	Mazda Driving Simulator	Serial	4	Japan
BMW [78]	BMW Driving Simulator	Parallel (Hexapod) + 2-axis linear rail	8	Germany
https://youtu.be/o-IKUa4d0Ok				
BMW	DiM250	Parallel	9	Germany
https://youtu.be/o-IKUa4d0Ok				
BMW	Delta	Hybrid	6	Germany
Mercedes-Benz [79]	MBS Driving Simulator	Parallel (Hexapod) + 1-axis linear rail	7	Germany
https://youtu.be/wdGsJkYv__A				
Continental AG	Delta	Hybrid	6	Germany
University of Iowa	NADS-1	Hybrid	8	United States
https://youtu.be/BvnXKHMh8qQ				
AB Dynamics	aVDS	Hybrid	6	United Kingdom
https://youtu.be/YH_mzFPdrYo				
Kempten University of Applied Sciences	aVDS	Hybrid	6	Germany
https://youtu.be/bHVnnMSIhUU				
Dynisma Motion Generators	DMG	Parallel	9	United Kingdom
Naval Medical Research Unit Dayton	KRAKEN	Serial	7	United States
https://youtu.be/E3Ex6_HdUHU				
NASA - Ames Research Center [45]	VMS	Hybrid	8	United States
TNO - Locatie Soesterberg/AMST-Systemtechnik	DESDEMONA	Serial	6	Netherlands
Eight360	Nova VR	Parallel	3	New Zealand
https://vimeo.com/395637826				
CKAS Mechatronics	CKAS W	Parallel	6	Australia
https://youtu.be/W757Kum3Cv0				
CKAS Mechatronics	CKAS WR	Hybrid	7	Australia
Dynamic Research, Inc	DRI Simulator	Parallel (Hexapod)	6	United States
Swedish National Road and Transport Research Institute (VTI) [80]	SIM IV	Parallel (Hexapod) + 2-axis linear rail	8	Sweden
Swedish National Road and Transport Research Institute (VTI) [48], [49]	SIM III	Serial	4	Sweden
Swedish National Road and Transport Research Institute (VTI)	SIM II	Serial	4	Sweden
Tongji University [81], [82]	TUDS	Parallel (Hexapod) + 2-axis linear rail	8	China
https://www.youtube.com/watch?v=ykeNQowcvpk				
Volvo Car Corporation	DiM250	Parallel	9	Sweden
https://www.youtube.com/watch?v=JzF9e7F1HWM&t=2s				
University of Stuttgart [83], [84]	Stuttgart Driving Simulator	Parallel (Hexapod) + 2-axis linear rail	8	Germany
KITE Institute for Rehabilitation Research	DriverLab	Parallel	6	Canada
https://youtu.be/ddy9-gdlcpM				
Reiser Simulation and Training GmbH	H145 Full Flight Simulator	Parallel	6	Germany
https://youtu.be/yiCzweT8OY4				
https://youtu.be/Kn-7klOr9Yg				
Motorcycle/Bicycle simulator				
Ansible Motion	Delta	Hybrid	7	United Kingdom
Cruden	MC1 motorcycle simulator	Parallel (Hexapod) + Steer	7	Netherlands
https://youtu.be/DHQYniah_GM				
Delft University	MOTORIST	Parallel	6	Netherlands
BMW [61]	Motorrad	Parallel (Hexapod) + Steer	7	Germany
Honda [85]	Honda Motorcycle Simulator	Parallel (Hexapod) + Steer	7	Japan
Würzburger Institut für Verkehrswissenschaften (WIVW) [61]	DESMORI	Parallel (Hexapod) + Steer	7	Germany
PERCRO Laboratory of the School of Advanced Studies of Pisa [60]	MORIS	Parallel (Hexapod) + Steer	7	Italy
Korea Advanced Institute of Science & Technology [86], [87]	KAIST Bicycle Simulator	Parallel (Hexapod) + Steer	7	South Korea

torque up to 80 Nm can be generated at the handlebar using an electrical actuator. The riders steer the motorcycle using a combination of steering torque and induced roll torque by shifting their weight. The two rear mirrors are simulated by 7'' TFT displays while the instrument cluster is represented by a 10'' TFT touchscreen containing a speedometer, revolution counter and gear indicator. Auditory feedback is provided by a helmet that has Sennheiser HD419 headphones installed. Additionally, a shaker placed beneath the seat transmits to the rider vibrations from the engine and high-frequency road roughness between 10 Hz to 50 Hz. Moreover, the rider is wearing a Motoair customized motorcycle airbag jacket with air-filled compartments. The jacket is attached to a system that pulls the rider backward while providing proprioceptive feedback on speed, acceleration, and static wind forces.

III. MOTION CUEING ALGORITHMS

In order to produce motion cues in driving simulators, a motion cueing algorithm is crucial. The angular velocity and linear acceleration of a vehicular system transform into the rotational and translational motions of a simulator within its physical constraints by using a motion cueing algorithm. The goal is to use the platform more effectively while adhering to its physical limitations by producing controlled motions with high levels of accuracy and fidelity. Consequently, there is a real need to reduce the sensation error between the simulator and real drivers, while satisfying the constraints imposed by the platform boundaries. The simulator must slow down and restrict its motion trajectory as the motion platform gets close to its physical workspace limits in order to remain inside these boundaries. Without any constraints in the MCA, the simulator acceleration could be contrary to the vehicle acceleration with a significant mismatch, causing the driver's expectation, inertial perceptions, and visual perceptions to feel inconsistent with each other. It is critical to handle the washout which is the transition of the simulator's states from tracking to braking action smoothly for both operational reasons (wear and tear) as well as for the safety of the simulator's occupants.

A. CLASSICAL WASHOUT FILTER

The classical algorithm [6], [7], [9], [10], [11], [12], [13] is the most widely used in commercial simulators. It is characterized by the empirically determined combination of linear high- and low-pass filters whose break frequencies and damping ratios can be adjusted off-line by trial and error. The schematic of this cueing technique is illustrated in Figure 5. Although the classical algorithm is mathematically and computationally simple and cheap, it uses linear elements and so does not fully exploit the simulator capabilities or fully take into account the nonlinear characteristics of human motion perception.

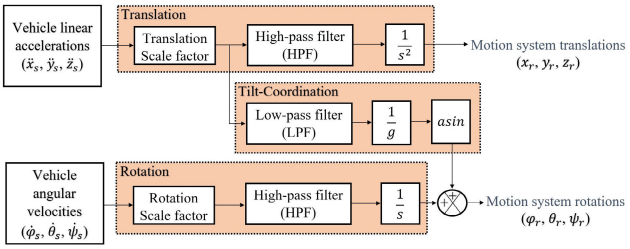

FIGURE 5. Classical washout filter motion cueing algorithm.

B. ADAPTIVE WASHOUT FILTER

There is an important advance between the classical washout filter motion cueing and an adaptive filter [6], [14], [15], [16], [17], which is the removal of erroneous rotational rate cues generated by classical filters. The adaptive washout filter's principle is the same as the classical one, with the main distinctions being that it uses nonlinear adaptive filters in lieu of linear ones, and it does the washout in the inertial reference frame as opposed to the body-axis system. Objective and subjective data were the focus of a comparative study in [14] between a linear classical washout filter technique and a nonlinear adaptive one. It appears that pilot performance as assessed was not affected by the motion cues during instrument-landing-system approaches for the objective experiments because there were no statistically significant variations in pilot performance for the various motion conditions. However, the subjective findings of this study suggest that the motion cues enhance the sense of realism. More importantly, the pilots expressly disapproved of aberrant rotational rate cues in roll and yaw with the linear technique, rating the nonlinear adaptive washout as considerably superior to the linear classical washout. The elimination of the unpleasant abnormal rate cues is extremely desirable in this situation since the pilots believed that roll representation to be the most crucial component of the overall airplane feel.

C. OPTIMAL WASHOUT FILTER

Reid and Nahon algorithm: The need to predict the sensation of actual physical motion by the human operator arises during the evaluation of motion-based drive algorithms and in the formulation of the optimal control algorithm [6]. Although many sensors throughout the human body play a role in this sensing process it is apparent that the vestibular system located in the head provides the dominant signals [88]. To obtain the desired time histories of sensation in response to a motion, dynamic models in the form of differential equations suitable for implementation on a digital computer are desirable. Such models have been developed and are reported in [89].

Sivan algorithm: In a dynamic flight motion simulator, the vestibular system plays a critical role in detecting motion cues. The otoliths and semicircular canals are two different groups of organs that constitute the vestibular system. It is

widely acknowledged [90], [91] that the semicircular canals play a significant role in both the detection of angular motion when light is not available as well as the detection of the high-frequency components of the angular motion even when light is present. The otoliths are also widely acknowledged [90], [91] to have a significant part in the detection of high-frequency components in the presence of light and the linear acceleration motion in the dark. Sivan [21] employed the optimal simulator design process based on the abovementioned assumptions to create the simulator motion in order to reduce the dissimilarity between the physiological outputs of the pilot's vestibular organs in the simulated scenario and those in an actual aircraft [92]. For this purpose, a weighted sum of the vestibular error which is the difference between the two pilots' otolith and semicircular outputs was kept at a minimum. The discrepancy between the motion cues in the actual aircraft and the moving simulator was measured using the mean-square value of vestibular error. In [21], the dynamical systems, including the vestibular systems, were modeled using time-invariant low-dimensional linearized equations.

ZyRo algorithm: When using washout algorithms in flight simulators, tilt coordination is utilized to demonstrate steady-state specific forces by rotating the motion platform to line up gravity with the overall specific force vector of the simulated aircraft. In the ZyRo algorithm [18], [19], a new tilt coordination control technique was established to be utilized with motion washout algorithms. Thus, a linear model of the tilt coordination system was introduced after removing the conventional linear high-pass filters from the classical washout algorithm. Furthermore, the tilt channel is controlled by a linear quadratic Gaussian regulator (LQGR) in a way that minimizes both the total position of the motion platform and the required tilt rate. Moreover, the required linear acceleration of the motion platform was decreased via nonlinear feedback to a level that could be controlled by the tilt channel control system. The outcome of these modifications is an adaptive complementary filter pair that offers unity gain and zero phase error for low-frequency and/or small specific force inputs. When inputs are large, the nonlinear feedback to the motion platform's required linear acceleration generates sagging cues that are reminiscent of those in the classical technique. In tests involving a set of deceleration maneuvers while taxiing, the ZyRo algorithm was found to outperform the classical washout filter technique.

Telban algorithm with Young Meiry vestibular model: The MCA introduced in [20] comprises models of the human vestibular sensory system, i.e. a unique semicircular canals model and the Young-Meiry otolith model [93], along with a new integrated vestibular-visual perception model. According to the Young-Meiry model of the functionality of the otolith receptors, otolith displacement causes hairs in sensory cells to deflect, which in return produces sensory signals. The otolith-endolymph system transforms a specific force input, such as tilt or linear acceleration, into the otolith displacement. Mechano-neural transduction system, which consists of sensory hair cells and both afferent and efferent neurons, further transforms this displacement into a sensory signal. An overdamped mass-spring-damper system could be used to model the otolith-endolymph system. Furthermore, due to losses in neural transmission and central nervous system processing, the quick dynamic response of the otolith will drop to the slower ocular torsion response.

D. OpDA ALGORITHM

OpDA algorithm was proposed by [22], which integrated dynamic models of the motion multi-sensory system, including the vestibular and the proprioceptive systems (Figure 6). OpDA showed to have a good response which tracks the target lateral specific force, decreases the false cues of angular velocity, and reduces the negative cues of head-tilted-angle. A comparison study shown in [22] illustrates that OpDA outperforms some of the current MCAs and offers performance at a level close to that of the MPC algorithm.

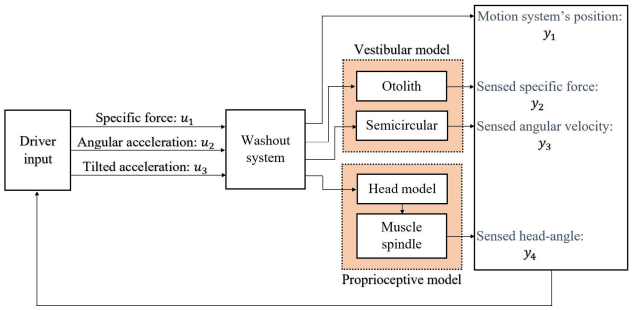

FIGURE 6. OpDA motion cueing algorithm.

E. SLIDING MODE-BASED CUEING

The aims of the classical sliding mode control technique are to control the state variables of an electro-mechanical system in such a way that they reach the sliding surface in the state space and then continue to slide along it to reach the origin ($s = 0$). This definition is adopted [23] and is utilized for the motion cueing purpose. The simulator thus has two operating modes. It starts in the washout filter motion cueing mode, generating motion references while moving inside the workspace. However, when the simulator reaches the working range limits, it then switches to sliding mode-based cueing if the prerequisites for sliding are met close to the sliding surface, and it remains in the sliding mode until the behavioral conflicts are settled.

F. MODEL PREDICTIVE CONTROL (MPC)

The MPC algorithm [24], [25], [26] minimizes a defined cost function in search of an optimal control law while taking into account the limitations of the system. In addition, it has the advantage of including the vestibular system of the human body, the Otolith model and the Semicircular canal model, which each is different by a specific transfer function

(Table 2). Figure 7 presents the block diagram of this cueing technique.

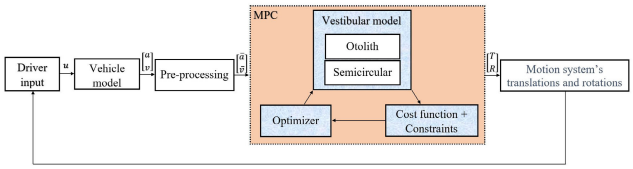

FIGURE 7. MPC motion cueing algorithm.

TABLE 2. Human vestibular models.

	Transfer function
Semicircular canal model	$\frac{\hat{\omega}}{\omega} = \frac{\tau_L \tau_a s^2 (1+\tau_1 s)}{(1+\tau_a s)(1+\tau_L s)(1+\tau_s s)}$
Otolith model	$\frac{\hat{f}}{f} = \frac{G_o(\tau_{ao} s+1)}{(\tau_{Lo} s+1)(\tau_{so} s+1)}$

In Table 2, ω and $\hat{\omega}$ are the real angular velocity and the perceived angular velocity for the three rotations around the x, y, z axes, respectively. Furthermore, f and $\hat{f}$ indicate the specific force and the sensed specific force, respectively. Based on the literature, the parameters for both Otolith and Semicircular canal models are largely determined by subjective responses and may change. Table 3 presents the parameters of the most popular vestibular models in MCAs.

TABLE 3. Parameters of vestibular models.

Model	Parameters							
	τ_L (sec)	τ_s (sec)	τ_1 (sec)	τ_a (sec)	G_o	τ_{ao} (sec)	τ_{Lo} (sec)	τ_{so} (sec)
[93], [94]	x: 6.1 y: 5.3 z: 10.2	0.1	0	30	0.4	13.2	5.33	0.66
[20]	5.73	0.005	0.06	80	0.4	10	5	0.016

G. TIME-VARYING MODEL PREDICTIVE CONTROL

Since the workspace on any motion platform is constrained, it is physically impossible to reproduce the actual vehicle signals. So, that is where the motion cueing algorithm plays its part by recreating a convincing vehicle motion feeling for the user within the physical and dynamic constraints of the motion platform. A Linear time-variant (LTV) MPC-based motion cueing algorithm [27], [28], [29] is introduced to overcome a common problem associated with linear time-invariant (LTI) MPC-based MCA methods. As discussed in III-F, the LTI MPC method is developed to obtain the best input motion signals while taking into account the motion platform constraints in the Cartesian coordinate system. However, this MCA is still unable to incorporate the design parameters of the motion platform mechanisms into their model, and handle any unexpected individual driver's behavior, which results in the occupant experiencing unrealistic motions. Due to this shortcoming, the LTV MPC-based MCA method is introduced which takes the design parameters of a motion platform alongside its physical constraints into consideration in the MPC model. Moreover, this MCA can be modified to the driving prowess of the particular user in order to obtain more accurate motion cues.

H. NONLINEAR MODEL PREDICTIVE CONTROL

Nonlinear model predictive motion cueing algorithm [30], [32] represented an improvement with respect to the linear algorithm described in [31] to handle the complex mechanical structure of a robotic-based simulator. It was shown that thorough the utilization of this algorithm a satisfactory performance can be achieved in terms of reproducing accurate perception even in critical operating conditions.

I. DEEP NEURAL NETWORK

A neural network can be utilized to imitate a motion cueing algorithm which provides optimal cueing (Figure 8). This method cannot be utilized to train a neural network in real-time experiments while there is a driver-in-the-loop because of the algorithm's offline nature. However, the neural network develops an approximation of an MCA after offline training that may be used with a driver-in-the-loop in real-time applications. In [33] (https://www.in.tum.de/fileadmin/w00bws/i06/Personal_Files/Emec_Ercelik/PMS_Final.mp4), the model was trained in an end-to-end manner, meaning that the neural network learned the complete next state of the simulator in addition to the control input signals. When applied to a dataset with a small sample size, the end-to-end approach produced more reliable results. In addition, a second cost term for neural network training was included to lessen the likelihood that learning the simulator's complete next state would result in inconsistent neural network outputs.

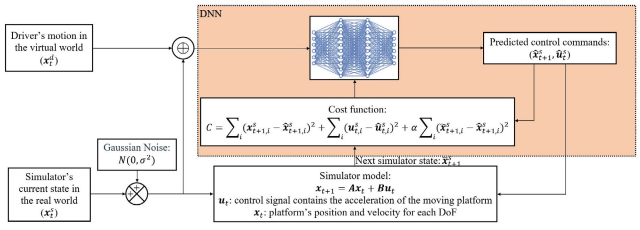

FIGURE 8. DNN motion cueing algorithm.

J. FUZZY CONTROL SYSTEM

Another type of MCAs is adaptive ones based on fuzzy logic [34] which have been used to replicate the motion signals of simulators. Considering the end-effector constraints in Cartesian space, it is claimed that the implementation of fuzzy logic-based adaptive MCA minimizes the movement sensation inaccuracy between the real vehicle and the simulation-based motion platform user. The schematic of this cueing technique is shown in Figure 9.

Unfortunately, motion cueing is widely believed to be the only part of the vehicular motion simulators contributing

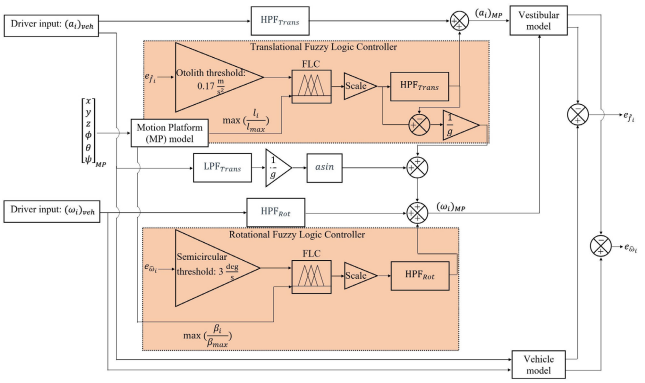

FIGURE 9. Fuzzy logic control motion cueing algorithm.

to the system's fidelity. However, the vehicle dynamic is deeply tied to the cueing definition, and it determines the sensation difference between the simulation environment and the real-world experience by the user. In the current state of motion cueing, including the abovementioned, the dynamic characteristics of the driven vehicle are ignored in the cueing algorithm. The changes in the dynamic characteristics of a vehicle result in retuning/redesigning of the motion cueing. In the future, more attention should be sought towards adapting vehicle dynamic parameters in the cueing algorithm, which not only can reduce the computation time when the vehicle model changes but also can improve the driver experience and the simulator's fidelity.

IV. CONTROL PARAMETERS TUNING METHODS

One issue associated with the development of MCAs for the generation of realistic motion for the vehicle's driver is the multitude of control parameters that require manual tuning in order to obtain the desired performance. Although trial and error is a possible solution, it is not recommended because it could jeopardize the system's safety. This approach opens the possibility that parameter combinations with high oscillation or instability could be chosen, resulting in the termination of the simulation. In addition, using such a method does not ensure the highest performance possible. Hence, an optimization technique must be used as a necessity to automate this process.

Generally speaking, optimization algorithms are divided into two types of algorithms: local and global search. Local search algorithms, particularly those based on gradients, have a high likelihood of trapping in local minima solutions, and their convergence is quite sensitive to chosen initial values. On the other hand, because of the derivative-free nature of global search algorithms, they are not affected by these drawbacks. In the literature, a number of global search algorithms have been proposed, including the Genetic Algorithm (GA) [95], Differential Evolution (DE) [96], Particle Swarm Optimization (PSO) [97], Spider Monkey Optimization (SMO) [98], Antlion optimization (ALO) [99], Grey wolf optimizer (GWO) [100], and many others. These algorithms send out a number of search agents into the solution space in an effort to find the optimization problem's global optima. These agents employ exploitation and exploration tactics to investigate their surroundings and identify the best and optimal solution. These tactics are necessary to prevent the local minima, which may cause an early convergence in some algorithms.

A. MEAN-VARIANCE MAPPING OPTIMIZATION (MVMO)

MVMO [101], [102], [103], [104], [105] is an emerging variant of a population-based, evolutionary optimization algorithm whose features include the evolution of its solutions through a unique search mechanism within a normalized range of the sample space. It uses a specific mapping function that is utilized to mutate the offspring based on the mean and variance of the n-best population achieved thus far. This mapping function always generates outputs that fall within the normalized range [0,1]. Consequently, this means that during the search process, the variable limits cannot be violated. Furthermore, MVMO updates the candidate solution around the best solution in each iteration step, adjusting the mapping curve's location and shape in accordance with the progress of the search process. Moreover, MVMO can swiftly locate the optimum with a low risk of premature convergence because of the carefully considered balance between search intensification and diversification.

B. GENETIC ALGORITHM (GA)

The GA-optimized nonlinear scaling unit [8], [106], [107], [108] is created to address the shortcomings of the existing scaling techniques, including the reliance on trial-and-error tuning, the inefficient workspace utilization, and the neglect of physical constraints and user perception factors in the scaling unit's design. By lowering human sensation error without breaching the simulator's physical constraints, the suggested nonlinear scaling unit can enhance the performance of optimal MCA.

C. PARTICLE SWARM OPTIMIZATION (PSO)

Particle swarm optimization (PSO) [97] is one of the population-based optimization algorithms inspired by believing that a school of fish or a flock of birds that moves in a group can profit from the experience of all other members. In PSO, a population of random solutions is used as the system's initial state, and subsequent generations are updated in order to find the optimal and best solution. In contrast to GA, PSO lacks evolution operators like mutation and crossover. In PSO, the particles—potential solutions—follow the current optimum particles as they move through the problem space. PSO is more efficient computationally in terms of memory and speed needs. PSO is unquestionably less precise and practical than GA, which are the evident drawbacks of this technique. Due to the advantages and disadvantages of the PSO technique, more researchers started to adopt a PSO-GA combined method for optimization [109], [110].

D. ANTLION OPTIMIZATION ALGORITHM

One of these metaheuristic optimization algorithms that is motivated by the biological behavior of antlions is the Antlion Optimizer (ALO), which was proposed/utilized in [99], [111], and [112]. Because it uses both local and global search for its exploitation and exploration stages, it has an edge over other algorithms. Through this combination, the search space is better explored and the optimal solution is found more quickly. Consequently, it has been applied to a variety of scientific problems, such as optimizing the control parameters for different kinds of engineering applications. The effectiveness of ALO in resolving a number of important optimization problems can be attributed to its simplicity and avoidance of local optima.

Table 4 highlights a summary of the state of existing MCAs and optimization algorithms.

TABLE 4. Summary table of the reviewed motion cueing and optimization algorithms.

Reference	Motion cueing algorithm
[6], [7], [9]–[13]	Classical washout filter
[6], [14]–[17]	Adaptive washout filter
[6], [18]–[21]	Optimal washout filter
[22]	OpDA algorithm
[23]	Sliding mode-based cueing
[24]–[26], [31]	Model predictive control
[27]–[29]	Time-varying model predictive control
[30], [32]	Nonlinear model predictive control
[33]	Neural network
[34]	Fuzzy control system
	Optimization algorithm
[8], [95], [106]–[108], [113], [114]	GA
[99], [111], [112]	ALO
[97]	PSO
[109], [110]	PSO-GA
[101]–[105]	MVMO
[98]	SMO
[100]	GWO
[96]	DE

V. CONCLUSION AND FUTURE WORK

This paper presented an in-depth review of dynamic motion simulator systems alongside the cueing and optimization algorithms that have been implemented to create comprehensive and realistic systems capable of mimicking the real-world experience for the driver. These advanced systems have evolved during the past few years and are utilized to simulate different types of scenarios including the land, air, and sea environments. The core of a motion simulator system consists of a robot that is capable of maneuvering in spatial space. This paper categorized these robotic machines based on their working principles and the number of DoF that they provide to facilitate smooth translational and rotational positioning in the 3d space. Furthermore, the control unit of these robotic machines contains a cueing algorithm in which the hyperparameters are optimally tuned utilizing an optimization technique. The current state of these cueing and optimization approaches was presented in this paper and the findings were outlined in Table 4.

Despite the advancement of these state-of-the-art systems, there are still works to be done in terms of performances and applications. The vehicle dynamic parameters should be integrated into the MCAs to improve the driving experience by the users and reduce the software computation time. This way the MCA will be dependent on the vehicle model and if the vehicle model changes, possibly only partial tunning of the MCAs is essential to be performed to obtain the optimal cueing algorithm and realistic driving experience. Furthermore, disturbance observers (DOs) have been proven to improve the performance of modern control techniques drastically [115], [116], [117]. DOs estimate external disturbances including wind, vibration, friction, temperature changes, inertial effects, and any unmodelled phenomena that can affect the motion of the simulator and generate compensation signals to counteract those effects. Therefore, it is expected by incorporating DOs into MCAs to improve the accuracy and realism of the motion simulators and lead to a more immersive experience. Moreover, tuning of MCAs' parameters is important for improving the overall performance of the motion simulator, particularly including motion/simulation sickness impacts on humans within them. Thus, a robust optimization procedure can improve the quality of the MCAs by finding the optimal solution for control parameters. Many of the existing optimization methods are prone to divergence and instability. To avoid this, robust optimization algorithms such as competitive gradient descent [118] can be considered in future works. This algorithm has shown to be less sensitive to the initial state of control parameters and with the ability to achieve faster convergence.

On the other hand, machine learning (ML) techniques such as Generative Adversarial Networks and Deep Learning [37], [38], [119], [120] could be utilized to create convincing artificial data or motion sickness compensation. In addition, future studies could investigate model-free Reinforcement Learning (RL) techniques integrated with modern control techniques such as model predictive control to get the advantages of both control schemes. By learning through exploration, the RL may be able to offer pre-trained neural networks that possess significantly higher-level and more reliable performance. Furthermore, with the development of AVs and, considering the complexity of our current road structures and the increased number of vehicles, it is important to look into smart vehicle platooning to minimize accident risks, transport times, costs, energy and fuel consumption. Using the simulator, and leveraging complex ML techniques, more in-depth V2X studies can be conducted [114]. Furthermore, existing real-world inefficient traffic light control causes numerous problems, such as long delays and waste of energy [121]. To improve efficiency, taking real-time traffic information as an input and dynamically adjusting the traffic light duration accordingly, is a key element which can help from the virtual environment of a simulator. Moreover, to deploy a large number of AVs in the future, safety and legal challenges need to be

overcome. To meet the necessary safety standards, effective collision avoidance technologies are required to ensure that the number of accidents is kept to a minimum. The research showed the implementation of ML techniques (e.g. Deep RL [122]) and modern control techniques (e.g. Multiconstrained MPC [123]) to train a controller that introduces collision avoidance behavior is a useful future activity. The use of simulation could further enhance previous achievements in these areas.

Furthermore, human factor analysis is an important part of vehicle manufacturing. Having a human in the loop of the process, the factors including drivers' age [124], [125], fatigue, level of concentration, level of comfort, risky driving, etc. have to be carefully studied [126] to improve regulations and legislation surrounding the vehicle's usage by the end-users. Besides, the cognitive load on the driver must be studied to examine the level of driver tiredness and fatigue, and differences that may arise between the simulation and real-world experiences. This information would improve results in an evaluation of the simulator's fidelity and realism.

Finally, the vehicle dynamics model needs to be as close as possible to the real vehicle to provide a complete sense of realism. Small details of a particular vehicle model may have a significant effect on the experience that is provided by driving a simulator. The suspension system, pedals' displacement-force relationship, seatbelt force, driver seat vibration, gear shift, steering wheel displacement-torque relationship, tire modelling, traction of the tire to the road surface under different road conditions, etc. are among the physics factors that need to be carefully studied and designed to not only provide an exceptional driving experience but also to increase the desirability, effectiveness and suitability of a commercial simulator.

Hopefully, the outcomes of this work will shed a light on the careful planning of further improvements in the future.

REFERENCES

[1] S. Kharrazi, B. Augusto, and N. Fröjd, "Vehicle dynamics testing in motion based driving simulators," *Vehicle Syst. Dyn.*, vol. 58, no. 1, pp. 92–107, 2020.

[2] A. O. Caffó, L. Tinella, A. Lopez, G. Spano, Y. Massaro, A. Lisi, F. Stasolla, R. Catanesi, F. Nardulli, I. Grattagliano, and A. Bosco, "The drives for driving simulation: A scientometric analysis and a selective review of reviews on simulated driving research," *Frontiers Psychol.*, vol. 11, p. 917, May 2020.

[3] ADAS Market. (2021). *ADAS Market by System (ACC, DMS, IPA, PDS, TJA, FCW, CTA, RSR, LDW, AEB, & BSD), Component (Radar, LiDAR, Ultrasonic, & Camera Unit), Vehicle (PC, LCV, Bus, & Truck), Level of Autonomy (L1, L2&3, L4, L5), Offering, EV, and Region—Global Forecast to 2030. MarketsAndMarkets*. Accessed: Oct. 19, 2022. [Online]. Available: https://www.marketsandmarkets.com/Market-Reports/driver-assistance-systems-market-1201.html

[4] A. L. Alexander, T. Brunyé, J. Sidman, and S. A. Weil, "From gaming to training: A review of studies on fidelity, immersion, presence, and buy-in and their effects on transfer in PC-based simulations and games," *DARWARS Training Impact Group*, vol. 5, pp. 1–14, Nov. 2005.

[5] W. A. Memon, I. Owen, and M. D. White, "Motion fidelity requirements for helicopter-ship operations in maritime rotorcraft flight simulators," *J. Aircr.*, vol. 56, no. 6, pp. 2189–2209, Nov. 2019.

[6] L. D. Reid and M. A. Nahon, "Flight simulation motion-base drive algorithms: Part 1. Developing and testing equations," UTIAS, Toronto, ON, Canada, Tech. Rep. 296, 1985.

[7] B. Conrad and S. F. Schmidt, "A study of techniques for calculating motion drive signals for flight simulators," Tech. Rep. NASA-CR-114345, 1971. [Online]. Available: https://ntrs.nasa.gov/citations/19710025909

[8] E. Thöndel, "Design and optimisation of a motion cueing algorithm for a truck simulator," in *Proc. 26th Annu. Eur. Simul. Model. Conf.*, Oct. 2012, vol. 22, no. 24, p. 10.

[9] M. Baarspul, "The generation of motion cues on a six-degrees-of-freedom motion system," Dept. Aerosp. Eng., Delft Univ. Technol., Delft, The Netherlands, Tech. Rep. LR-248, 1977.

[10] R. V. Parrish, J. E. Dieudonne, and D. J. Martin, "Motion software for a synergistic six-degree-of-freedom motion base," Nat. Aeronaut. Space Admin., Washington, DC, USA, Tech. Rep. NASA-TN-D-7350, 1973.

[11] B. Conrad and S. F. Schmidt, "Motion drive signals for piloted flight simulators," Tech. Rep., 1970. [Online]. Available: https://ntrs.nasa.gov/citations/19700017803

[12] P. R. Grant and L. D. Reid, "Motion washout filter tuning: Rules and requirements," *J. Aircr.*, vol. 34, no. 2, pp. 145–151, Mar. 1997.

[13] F. Barbagli, D. Ferrazzin, C. A. Avizzano, and M. Bergamasco, "Washout filter design for a motorcycle simulator," in *Proc. IEEE Virtual Reality*, Aug. 2001, pp. 225–232.

[14] R. V. Parrish and D. J. Martin Jr., "Comparison of a linear and a nonlinear washout for motion simulators utilizing objective and subjective data from CTOL transport landing approaches," Tech. Rep. NASA TN D-8157, L-10593, Washington, DC, USA, 1976.

[15] R. Parrish, J. Dieudonne, R. Bowles, and D. Martin Jr., "Coordinated adaptive filters for motion simulators," in *Proc. Vis. Motion Simul. Conf.*, Sep. 1973, pp. 295–300.

[16] R. V. Parrish, J. E. Dieudonne, R. L. Bowles, and D. J. Martin, "Coordinated adaptive washout for motion simulators," *J. Aircr.*, vol. 12, no. 1, pp. 44–50, Jan. 1975.

[17] R. Parrish and D. Martin Jr., "Empirical comparison of a linear and a nonlinear washout for motion simulators," in *Proc. 13th Aerosp. Sci. Meeting*, Jan. 1975, p. 106.

[18] H. J. Zywiol and R. Romano, "Motion drive algorithms and simulator design to study motion effects on infantry soldiers," Army Tank Automot. Res. Develop. Eng. Center, Warren, MI, USA, Tech. Rep., 2003. [Online]. Available: https://apps.dtic.mil/sti/citations/ADA572240

[19] R. Romano, "Non-linear optimal tilt coordination for washout algorithms," in *Proc. AIAA Model. Simul. Technol. Conf. Exhibit*, Aug. 2003, p. 5681.

[20] R. J. Telban and F. M. Cardullo, "Motion cueing algorithm development: Human-centered linear and nonlinear approaches," Tech. Rep. NASA/CR-2005-213747, 2005. [Online]. Available: https://ntrs.nasa.gov/citations/20050180246

[21] R. Sivan, J. Ish-Shalom, and J.-K. Huang, "An optimal control approach to the design of moving flight simulators," *IEEE Trans. Syst., Man, Cybern.*, vol. SMC-12, no. 6, pp. 818–827, Nov. 1982.

[22] P. Duc-An and N. Duc-Toan, "A novel motion cueing algorithm integrated multi-sensory system–vestibular and proprioceptive system," *Proc. Inst. Mech. Engineers, K, J. Multi-Body Dyn.*, vol. 234, no. 2, pp. 256–271, Jun. 2020.

[23] A. Sharma, M. S. Ikbal, D. T. Cuong, and M. Zoppi, "A sliding mode-based approach to motion cueing for virtual reality gaming using motion simulators," *Virtual Reality*, vol. 25, no. 1, pp. 95–106, Mar. 2021.

[24] M. Soyer, S. Olaru, and Z. Fang, "A novel motion cueing algorithm based on real-time optimization and periodic invariant sets," in *Proc. IEEE Conf. Control Technol. Appl. (CCTA)*, Aug. 2020, pp. 19–24.

[25] M. Bruschetta, D. L. Mendola, A. Beghi, and D. Minen, "An MPC based motion cueing algorithm with side slip dynamics," in *Proc. Driving Simul. Conf. Europe*, Antibes, France, 2018, pp. 1–5.

[26] Z. Fang and A. Kemeny, "An efficient model predictive control-based motion cueing algorithm for the driving simulator," *Simulation*, vol. 92, no. 11, pp. 1025–1033, Nov. 2016.

[27] F. Maran, M. Bruschetta, A. Beghi, and D. Minen, "Improvement of an MPC-based motion cueing algorithm with time-varying prediction and driver behaviour estimation," in *Proc. Driving Simul. Conf.*, Sep. 2015, pp. 16–18.

[28] M. R. C. Qazani, H. Asadi, S. Khoo, and S. Nahavandi, "A linear time-varying model predictive control-based motion cueing algorithm for hexapod simulation-based motion platform," *IEEE Trans. Syst., Man, Cybern. Syst.*, vol. 51, no. 10, pp. 6096–6110, Oct. 2021.

[29] M. R. Chalak Qazani, H. Asadi, S. Mohamed, C. P. Lim, and S. Nahavandi, "A time-varying weight MPC-based motion cueing algorithm for motion simulation platform," *IEEE Trans. Intell. Transp. Syst.*, vol. 23, no. 8, pp. 11767–11778, Aug. 2022.

[30] M. Bruschetta, F. Maran, and A. Beghi, "A nonlinear, MPC-based motion cueing algorithm for a high-performance, nine-DOF dynamic simulator platform," *IEEE Trans. Control Syst. Technol.*, vol. 25, no. 2, pp. 686–694, Mar. 2017.
[31] A. Beghi, M. Bruschetta, and F. Maran, "A real time implementation of MPC based motion cueing strategy for driving simulators," in *Proc. IEEE 51st IEEE Conf. Decis. Control (CDC)*, Dec. 2012, pp. 6340–6345.
[32] M. Katliar, J. Fischer, G. Frison, M. Diehl, H. Teufel, and H. H. Bülthoff, "Nonlinear model predictive control of a cable-robot-based motion simulator," *IFAC-PapersOnLine*, vol. 50, no. 1, pp. 9833–9839, Jul. 2017.
[33] A. B. Koyuncu, E. Ercelik, E. Comulada-Simpson, J. Venrooij, M. Kaboli, and A. Knoll, "A novel approach to neural network-based motion cueing algorithm for a driving simulator," in *Proc. IEEE Intell. Vehicles Symp. (IV)*, Oct. 2020, pp. 2118–2125.
[34] M. R. Chalak Qazani, H. Asadi, T. Bellmann, S. Perdrammehr, S. Mohamed, and S. Nahavandi, "A new fuzzy logic based adaptive motion cueing algorithm using parallel simulation-based motion platform," in *Proc. IEEE Int. Conf. Fuzzy Syst. (FUZZ-IEEE)*, Jul. 2020, pp. 1–8.
[35] F. Ellensohn, M. Spannagl, S. Agabekov, J. Venrooij, M. Schwienbacher, and D. Rixen, "A hybrid motion cueing algorithm," *Control Eng. Pract.*, vol. 97, Apr. 2020, Art. no. 104342.
[36] D. A. Pham and D. T. Nguyen, "False cue influence on motion cue quality for 10 motion cueing algorithms," *Sci. Prog.*, vol. 104, no. 3, 2021, Art. no. 00368504211036857.
[37] S. Hell and V. Argyriou, "Machine learning architectures to predict motion sickness using a virtual reality rollercoaster simulation tool," in *Proc. IEEE Int. Conf. Artif. Intell. Virtual Reality (AIVR)*, Dec. 2018, pp. 153–156.
[38] C.-Y. Liao, S.-K. Tai, R.-C. Chen, and H. Hendry, "Using EEG and deep learning to predict motion sickness under wearing a virtual reality device," *IEEE Access*, vol. 8, pp. 126784–126796, 2020.
[39] T. Adachi, T. Yonekawa, Y. Fuwamoto, S. Ito, K. Iwazaki, and S. Nagiri, "Simulator motion sickness evaluation based on eye mark recording during vestibulo-ocular reflex," SAE, Warrendale, PA, USA, Tech. Paper 2014-01-0441, 2014.
[40] T. Irmak, K. N. de Winkel, D. M. Pool, H. H. Bülthoff, and R. Happee, "Individual motion perception parameters and motion sickness frequency sensitivity in fore-aft motion," *Exp. Brain Res.*, vol. 239, no. 6, pp. 1727–1745, Jun. 2021.
[41] L. Guo, F. Cardullo, J. Houck, L. Kelley, and T. Wolters, "New predictive filters for compensating the transport delay on a flight simulator," in *Proc. AIAA Model. Simul. Technol. Conf. Exhibit*, Aug. 2004, p. 5441.
[42] L. Guo, F. Cardullo, J. Houck, L. Kelley, and T. Wolters, "A comprehensive study of three delay compensation algorithms for flight simulators," in *Proc. AIAA Model. Simul. Technol. Conf. Exhibit*, Aug. 2005, p. 5896.
[43] F. Saidi, G. Millet, and G. Galle, "Transport delay characterization of scaner driving simulator," in *Proc. Driving Simulator Conf. Europe*, Aug. 2010, pp. 89–97.
[44] R. M. Smith, V. I. Chung, and D. Martinez, "Transport delays associated with NASA Langley flight simulation facility," Tech. Rep. NASA-TM-110150, 1995. [Online]. Available: https://ntrs.nasa.gov/citations/19950023033
[45] B. L. Aponso, S. D. Beard, and J. A. Schroeder, "The NASA Ames vertical motion simulator—A facility engineered for realism," in *Proc. Roy. Aeronaut. Soc. Spring Flight Simul. Conf.*, Jun. 2009, p. 4.
[46] A. Berthoz, "Motion scaling for high-performance driving simulators," *IEEE Trans. Human-Mach. Syst.*, vol. 43, no. 3, pp. 265–276, May 2013.
[47] A. W. Stedmon, B. Hasseldine, D. Rice, M. Young, S. Markham, M. Hancox, E. Brickell, and J. Noble, "'MotorcycleSim': An evaluation of rider interaction with an innovative motorcycle simulator," *Comput. J.*, vol. 54, no. 7, pp. 1010–1025, Jul. 2011.
[48] C. Ahlstrm, A. Bolling, G. Srensen, O. Eriksson, and A. Andersson, "Validating speed and road surface realism in VTI driving simulator III," Statens vg-och transportforskningsinstitut, Tech. Rep., 2012. [Online]. Available: http://vti.diva-portal.org/smash/record.jsf?pid=diva2%3A670642&dswid=-9072
[49] A. Bolling, J. Jansson, M. Hjort, M. Lidstroöm, S. Nordmark, H. Sehammar, and L. Sjoögren, "An approach for realistic simulation of real road condition in a moving base driving simulator," *J. Comput. Inf. Sci. Eng.*, vol. 11, no. 4, 2011, Art. no. 041006.
[50] T. Bellmann, J. Heindl, M. Hellerer, R. Kuchar, K. Sharma, and G. Hirzinger, "The DLR robot motion simulator part I: Design and setup," in *Proc. IEEE Int. Conf. Robot. Autom.*, May 2011, pp. 4694–4701.
[51] T. Bellmann, M. Otter, and G. Hirzinger, "The DLR robot motion simulator part II: Optimization based path-planning," in *Proc. IEEE Int. Conf. Robot. Autom.*, May 2011, pp. 4702–4709.
[52] Y. Nie, T. Bellmann, A. Labusch, G. Looye, E.-J. Van Kampen, and Q. P. Chu, "Aircraft upset and recovery simulation with the DLR robot motion simulator," in *Proc. AIAA Model. Simul. Technol. Conf.*, Jan. 2015, p. 1142.
[53] P. R. Giordano, C. Masone, J. Tesch, M. Breidt, L. Pollini, and H. H. Bülthoff, "A novel framework for closed-loop robotic motion simulation—Part I: Inverse kinematics design," in *Proc. IEEE Int. Conf. Robot. Autom.*, May 2010, pp. 3876–3883.
[54] Y. R. Khusro, Y. Zheng, M. Grottoli, and B. Shyrokau, "MPC-based motion-cueing algorithm for a 6-DOF driving simulator with actuator constraints," *Vehicles*, vol. 2, no. 4, pp. 625–647, Dec. 2020.
[55] O. Stroosma, M. M. van Paassen, and M. Mulder, "Using the SIMONA research simulator for human–machine interaction research," in *Proc. AIAA Model. Simul. Technol. Conf. Exhibit*, Aug. 2003, p. 5525.
[56] N. Kovácsová, M. Grottoli, F. Celiberti, Y. Lemmens, R. Happee, M. P. Hagenzieker, and J. C. F. de Winter, "Emergency braking at intersections: A motion-base motorcycle simulator study," *Appl. Ergonom.*, vol. 82, Jan. 2020, Art. no. 102970.
[57] B. E. Westerhof, E. J. H. de Vries, R. Happee, and A. Schwab, "Evaluation of a motorcycle simulator," in *Proc. Symp. Dynamics Control Single Track Vehicles*, Jan. 2020, pp. 1–21.
[58] B. Westerhof, "Evaluation of the Cruden motorcycle simulator," Tech. Rep., 2018. [Online]. Available: https://repository.tudelft.nl/islandora/object/uuid%3A05a77692-ed92-4d85-8bc1-0f0038babf12
[59] F. Colombet, Z. Fang, and A. Kemeny, "Pitch tilt rendering for an 8-DOF driving simulator," DSC, Tech. Rep., 2015. [Online]. Available: https://hal.science/hal-01948450/
[60] D. Ferrazzin, F. Salsedo, F. Barbagli, C. A. Avizzano, G. Di Pietro, A. Brogni, M. Vignoni, and M. Bergamasco, "The Moris motorcycle simulator: An overview," *SAE Trans.*, pp. 199–210, 2002. [Online]. Available: https://saemobilus.sae.org/content/2001-01-1874/ and https://www.jstor.org/stable/pdf/44743052.pdf?casa_token=ZyCjrJUboCAAAAAA:a-ojm4dmBDIszgQU3VXr82oS–Jl3Yuh0ssIxYI7YufOOB0Ow54jYiY8r4ooGhQfu0_x4PNKoBbnGtRMgI_nzwWNBPm3QV95lDHO8E7APT5tTd2IKNbG
[61] S. Will, R. Ple, and S. Guth, "Bringing single track vehicle dynamics to motorcycle riding simulators–results of a pilot study," *Proc., Bicycle Motorcycle Dyn.*, 2016. [Online]. Available: https://figshare.com/articles/journal_contribution/Bringing_single_track_vehicle_dynamics_to_motorcycle_riding_simulators_-_results_of_a_pilot_study/3851736?backTo=/collections/Proceedings_of_the_2016_Bicycle_and_Motorcycle_Dynamics_Conference/3460590
[62] M. Blommer, "Ford's use of driving simulator technology for automated driving feature development," in *Proc. Driving Simul. Virtual Reality Conf. Exhib.*, Sep. 2018, pp. 1–20.
[63] F. Cheli, A. Fossati, and G. Mastinu, "Enhanced immersive reality through cable-driven simulators," *ATZ Worldwide*, vol. 123, no. 10, pp. 58–61, Oct. 2021.
[64] S. Nahavandi, Z. Najdovski, and A. Bhatti, *Universal Motion Simulator*, U.S. Patent US1 087 518 8B2, Dec. 29, 2020.
[65] S. Nahavandi, "Robot-based motion simulators using washout filtering: Dynamic, immersive land, air, and sea vehicle training, vehicle virtual prototyping, and testing," *IEEE Syst., Man, Cybern. Mag.*, vol. 2, no. 3, pp. 6–10, Jul. 2016.
[66] N. Mohajer, H. Asadi, S. Nahavandi, and C. P. Lim, "Evaluation of the path tracking performance of autonomous vehicles using the universal motion simulator," in *Proc. IEEE Int. Conf. Syst., Man, Cybern. (SMC)*, Oct. 2018, pp. 2115–2121.
[67] R. Stevens and K. Cammaerts, *Mobile Platform*, CA Patent CA27 769 86C, Dec. 17, 2013.
[68] R. Stevens and K. Cammaerts, *Motion Platform Apparatus and Method of Supporting a Payload Platform*, GB Patent GB26 023 51A, Jun. 29, 2022.
[69] K. Cammaerts, P. Morse, and K. Kidera, "Improving performance through the use of driver-in-the-loop simulations," *ATZ worldwide*, vol. 121, no. 1, pp. 52–57, Jan. 2019.
[70] O. X. Kuiper, J. E. Bos, C. Diels, and K. Cammaerts, "Moving base driving simulators' potential for carsickness research," *Appl. Ergonom.*, vol. 81, Nov. 2019, Art. no. 102889.
[71] J. A. Greenberg and T. J. Park, "The Ford driving simulator," SAE, Warrendale, PA, USA, Tech. Paper 940176, 1994.
[72] P. R. Giordano, C. Masone, J. Tesch, M. Breidt, L. Pollini, and H. H. Bülthoff, "A novel framework for closed-loop robotic motion simulation—Part II: Motion cueing design and experimental validation," in *Proc. IEEE Int. Conf. Robot. Autom.*, May 2010, pp. 3896–3903.

[73] T. Denoual, F. Mars, J. F. Petiot, and A. Kemeny, "Toward predicting the subjective assessment of ESC in a driving simulator," in *Proc. Driving Simul. Conf. Europe (DSC) Les Collections de l'IFSTTAR*, 2012, pp. 289–298.

[74] C. Rengifo, J.-R. Chardonnet, H. Mohellebi, and A. Kemeny, "Impact of human-centered vestibular system model for motion control in a driving simulator," *IEEE Trans. Hum.-Mach. Syst.*, vol. 51, no. 5, pp. 411–420, Oct. 2021.

[75] R. Suikat, "The new dynamic driving simulator at DLR," in *Proc. Driving Simulator Conf.*, no. 8, Nov. 2005, pp. 374–381.

[76] M. Fischer, A. Richter, J. Schindler, J. Plttner, G. Temme, J. Kelsch, D. Assmann, and F. Kster, "Modular and scalable driving simulator hardware and software for the development of future driver assistence and automation systems," in *Proc. New Develop. Driving Simul. Design Exp.*, 2014, pp. 223–229.

[77] T. Suetomi, A. Horiguchi, Y. Okamoto, and S. Hata, "The driving simulator with large amplitude motion system," *SAE Trans.*, pp. 94–101, 1991. [Online]. Available: https://www.jstor.org/stable/44632016

[78] *Two Projection Systems for BMW High-Fidelity and High-Dynamic Driving Simulators*. Accessed: Mar. 16, 2023. [Online]. Available: https://www.project-syntropy.de/wp-content/uploads/2021/10/BMW-HF-BMW-HD-Driving-Simulators.pdf

[79] *Visual Display System Renewal for Daimler AG MBS Moving-Base Driving Simulator*. Accessed: Mar. 16, 2023. [Online]. Available: https://www.project-syntropy.de/wp-content/uploads/2021/05/Daimler-MBS-Simulator.pdf

[80] J. Jansson, J. Sandin, B. Augusto, M. Fischer, B. Blissing, and L. Kllgren, "Design and performance of the VTI Sim IV," in *Proc. Driving Simul. Conf.*, Sep. 2014, pp. 128–138.

[81] X. Wang, M. Chen, M. Zhu, and P. Tremont, "Development of a kinematic-based forward collision warning algorithm using an advanced driving simulator," *IEEE Trans. Intell. Transp. Syst.*, vol. 17, no. 9, pp. 2583–2591, Sep. 2016.

[82] Y. Wang, X. Yang, L. Huang, and J. Wang, "Lane-level vehicle trajectory reckoning for cooperative vehicle-infrastructure system," *Discrete Dyn. Nature Soc.*, vol. 2012, pp. 1–15, 2012.

[83] T. Miunske, C. Holzapfel, E. Baumgartner, and H.-C. Reuss, "A new approach for an adaptive linear quadratic regulated motion cueing algorithm for an 8 DoF full motion driving simulator," in *Proc. Int. Conf. Robot. Autom. (ICRA)*, May 2019, pp. 497–503.

[84] G. Baumann, T. Riemer, C. Liedecke, P. Rumbolz, and A. Schmidt, "How to build Europe's largest eight-axes motion simulator," in *Proc. Driving Simul. Conf., Driving Simul. Assoc.*, Sep. 2012, pp. 1–2.

[85] S. Chiyoda, K. Yoshimoto, D. Kawasaki, Y. Murakami, and T. Sugimoto, "Development of a motorcycle simulator using parallel manipulator and head mounted display," in *Proc. Int. Conf. Motion Vib. Control Japan Soc. Mech. Eng.*, 2002, pp. 599–602.

[86] D. S. Kwon, G. H. Yang, C. W. Lee, J. C. Shin, Y. Park, B. Jung, D. Y. Lee, K. Lee, S. H. Han, B. H. Yoo, and K. Y. Wohn, "KAIST interactive bicycle simulator," in *Proc. IEEE Int. Conf. Robot. Automat.*, vol. 3, May 2001, pp. 2313–2318.

[87] J.-C. Shin and C.-W. Lee, "Rider's net moment estimation using control force of motion system for bicycle simulator," *J. Robotic Syst.*, vol. 21, no. 11, pp. 597–607, Nov. 2004.

[88] D. R. Gum, "Modeling of the human force and motion-sensing mechanics," Air Force Human Resour. Lab., Tech. Rep., 1973. [Online]. Available: https://apps.dtic.mil/sti/citations/AD0766444

[89] G. L. Zacharias, "Motion cue models for pilot-vehicle analysis," Bolt Beranek and Newman, Control Syst. Dept., Cambridge, MA, USA, Tech. Rep., 1978. [Online]. Available: https://apps.dtic.mil/sti/citations/ADA061477

[90] F. E. Guedry, "Psychophysics of vestibular sensation. in *Vestibular System Part 2: Psychophysics, Applied Aspects and General Interpretations*. Berlin, Germany: Springer, 1974, pp. 3–154.

[91] R. A. Peters, "Dynamics of the vestibular system and their relation to motion perception, spatial disorientation, and illusions," Nat. Aeronaut. Space Admin., Washington, DC, USA, Tech. Rep., 1969, pp. 1–168. [Online]. Available: https://ntrs.nasa.gov/citations/19690013275

[92] R. J. A. W. Hosman, J. C. Van der Vaart, and G. A. van de Moesdijk, "Optimalization and evaluation of linear motion filters," Delft Univ. Technol., Delft, The Netherlands, Tech. Rep., 1979. [Online]. Available: https://www.researchgate.net/publication/309151953_OPTIMALIZATION_AND_EVALUATION_OF_LINEAR_MOTION_FILTERS

[93] L. R. Young and J. L. Meiry, "A revised dynamic otolith model," *Aerosp. Med.*, vol. 39, no. 6, pp. 606–608, 1968.

[94] L. R. Young and C. M. Oman, "Model for vestibular adaptation to horizontal rotation," *Aerosp. Med.*, vol. 40, no. 10, pp. 1076–1080, 1969.

[95] M. Mitchell. *An Introduction to Genetic Algorithms*. Cambridge, MA, USA: MIT Press, 1998.

[96] K. Price, R. M. Storn, and J. A. Lampinen, *Differential Evolution: A Practical Approach to Global Optimization*. Berlin, Germany: Springer, 2006.

[97] J. Kennedy and R. C. Eberhart, "Particle swarm optimization," in *Proc. IEEE Int. Conf. Neural Netw.*, vol. 4, Nov./Dec. 1995, pp. 1942–1948.

[98] J. C. Bansal, H. Sharma, S. S. Jadon, and M. Clerc, "Spider monkey optimization algorithm for numerical optimization," *Memetic Comput.*, vol. 6, no. 1, pp. 31–47, Mar. 2014.

[99] S. Mirjalili, "The ant lion optimizer," *Adv. Eng. Softw.*, vol. 83, pp. 80–98, May 2015.

[100] S. Mirjalili, S. M. Mirjalili, and A. Lewis, "Grey wolf optimizer," *Adv. Eng. Softw.*, vol. 69, pp. 46–61, Mar. 2014.

[101] I. Erlich, G. K. Venayagamoorthy, and N. Worawat, "A mean-variance optimization algorithm," in *Proc. IEEE Congr. Evol. Comput.*, Jul. 2010, pp. 1–6.

[102] H. V. Pham, J. L. Rueda, and I. Erlich, "Online optimal control of reactive sources in wind power plants," *IEEE Trans. Sustain. Energy*, vol. 5, no. 2, pp. 608–616, Apr. 2014.

[103] T. Guo and J. V. Milanović, "Probabilistic framework for assessing the accuracy of data mining tool for online prediction of transient stability," *IEEE Trans. Power Syst.*, vol. 29, no. 1, pp. 377–385, Jan. 2014.

[104] D. A. Pham "Mean-variance mapping optimization for auto-tuning parameters of classical motion cueing algorithm," in *Proc. Int. Conf. Mater., Mach. Methods Sustainable Develop.* Cham, Switzerland: Springer, pp. 952–957.

[105] D. A. Pham and D. T. Nguyen, "Auto-tuning parameters of motion cueing algorithms for high performance driving simulator based on Kuka Robocoaster," *Sci. Prog.*, vol. 105, no. 2, 2022, Art. no. 368504221104333.

[106] H. Asadi, C. P. Lim, A. Mohammadi, S. Mohamed, S. Nahavandi, and L. Shanmugam, "A genetic algorithm-based nonlinear scaling method for optimal motion cueing algorithm in driving simulator," *Proc. Inst. Mech. Eng., I, J. Syst. Control Eng.*, vol. 232, no. 8, pp. 1025–1038, 2018.

[107] H. Asadi, S. Mohamed, C. P. Lim, and S. Nahavandi, "Robust optimal motion cueing algorithm based on the linear quadratic regulator method and a genetic algorithm," *IEEE Trans. Syst., Man, Cybern., Syst.*, vol. 47, no. 2, pp. 238–254, Feb. 2017.

[108] H. Asadi, S. Mohamed, D. R. Zadeh, and S. Nahavandi, "Optimisation of nonlinear motion cueing algorithm based on genetic algorithm," *Veh. Syst. Dyn.*, vol. 53, no. 4, pp. 526–545, 2015.

[109] X. H. Shi, Y. C. Liang, H. P. Lee, C. Lu, and L. M. Wang, "An improved GA and a novel PSO-GA-based hybrid algorithm," *Inf. Process. Lett.*, vol. 93, no. 5, pp. 255–261, Mar. 2005.

[110] B. Jamali, M. Rasekh, F. Jamadi, R. Gandomkar, and F. Makiabadi, "Using PSO-GA algorithm for training artificial neural network to forecast solar space heating system parameters," *Appl. Thermal Eng.*, vol. 147, pp. 647–660, Jan. 2019.

[111] S. Mouassa, T. Bouktir, and A. Salhi, "Ant lion optimizer for solving optimal reactive power dispatch problem in power systems," *Eng. Sci. Technol. Int. J.*, vol. 20, no. 3, pp. 885–895, Jun. 2017.

[112] A. A. L. Al-Jodah, B. Shirinzadeh, J. Pinskier, M. Ghafarian, T. K. Das, Y. Tian, and D. Zhang, "Antlion optimized robust control approach for micropositioning trajectory tracking tasks," *IEEE Access*, vol. 8, pp. 220889–220907, 2020.

[113] M. Jones, "Motion cueing optimisation applied to rotorcraft flight simulation," *CEAS Aeronaut. J.*, vol. 8, no. 3, pp. 523–539, Sep. 2017.

[114] S. Prathiba, G. Raja, K. Dev, N. Kumar, and M. Guizani, "A hybrid deep reinforcement learning for autonomous vehicles smart-platooning," *IEEE Trans. Veh. Technol.*, vol. 70, pp. 13340–13350, 2021.

[115] M. Ghafarian, B. Shirinzadeh, A. Al-Jodah, T. K. Das, and T. Shen, "Experimental system identification and disturbance observer-based control for a monolithic $Z\theta_x\theta_y$ precision positioning system," 2023 *arXiv:2301.05358*.

[116] A. Al-Jodah, B. Shirinzadeh, M. Ghafarian, T. K. Das, Y. Tian, and D. Zhang, "A fuzzy disturbance observer based control approach for a novel 1-DOF micropositioning mechanism," *Mechatronics*, vol. 65, Feb. 2020, Art. no. 102317.

[117] A. Al-Jodah, B. Shirinzadeh, M. Ghafarian, T. K. Das, J. Pinskier, Y. Tian, and D. Zhang, "Modeling and a cross-coupling compensation control methodology of a large range 3-DOF micropositioner with low parasitic motions," *Mechanism Mach. Theory*, vol. 162, Aug. 2021, Art. no. 104334.

[118] F. Schäfer and A. Anandkumar, "Competitive gradient descent," 2019, *arXiv:1905.12103*.
[119] N. Padmanaban, T. Ruban, V. Sitzmann, A. M. Norcia, and G. Wetzstein, "Towards a machine-learning approach for sickness prediction in 360° stereoscopic videos," *IEEE Trans. Vis. Comput. Graph.*, vol. 24, no. 4, pp. 1594–1603, Apr. 2018.
[120] P. M. Kebria, A. Khosravi, S. M. Salaken, and S. Nahavandi, "Deep imitation learning for autonomous vehicles based on convolutional neural networks," *IEEE/CAA J. Autom. Sinica*, vol. 7, no. 1, pp. 82–95, Jan. 2020.
[121] X. Liang, X. Du, G. Wang, and Z. Han, "A deep Q learning network for traffic lights' cycle control in vehicular networks," *IEEE Trans. Veh. Technol.*, vol. 68, no. 2, pp. 1243–1253, Jan. 2019.
[122] S. Na, H. Niu, B. Lennox, and F. Arvin, "Bio-inspired collision avoidance in swarm systems via deep reinforcement learning," *IEEE Trans. Veh. Technol.*, vol. 71, no. 3, pp. 2511–2526, Mar. 2022.
[123] J. Ji, A. Khajepour, W. W. Melek, and Y. Huang, "Path planning and tracking for vehicle collision avoidance based on model predictive control with multiconstraints," *IEEE Trans. Veh. Technol.*, vol. 66, no. 2, pp. 952–964, Apr. 2016.
[124] F. Hartwich, M. Beggiato, and J. F. Krems, "Driving comfort, enjoyment and acceptance of automated driving–effects of drivers' age and driving style familiarity," *Ergonomics*, vol. 61, no. 8, pp. 1017–1032, Aug. 2018.
[125] J. R. G. Kuniyoshi, A. T. Costa, A. Cruz Figueira, F. I. Kabbach, and A. P. C. Larocca, "Driver's visual perception as a function of age. Using a driving simulator to explore driver's eye movements in vertical signs," *Transp. Res. Interdiscipl. Perspect.*, vol. 11, Sep. 2021, Art. no. 100460.
[126] J. Michaels, R. Chaumillon, D. Nguyen-Tri, D. Watanabe, P. Hirsch, F. Bellavance, G. Giraudet, D. Bernardin, and J. Faubert, "Driving simulator scenarios and measures to faithfully evaluate risky driving behavior: A comparative study of different driver age groups," *PLoS ONE*, vol. 12, no. 10, Oct. 2017, Art. no. e0185909.

MOHAMMADALI GHAFARIAN (Member, IEEE) received the Ph.D. degree in robotics and mechatronics from Monash University, in 2021. He is currently working on establishing the next-generation of vehicular motion simulator with the Institute for Intelligent Systems Research and Innovation (IISRI), Deakin University, Australia. His current research interests include robotic systems, robust/adaptive control system designs, real-time systems, sensor fusion, and finite element modeling. He was a member of the Robotics and Mechatronics Research Laboratory (RMRL). He is a member of the Institution of Engineers Australia (MIEAust).

MATTHEW WATSON received the Ph.D. degree from Deakin University, in 2013. He is currently a Senior Research Fellow in mechatronics systems modeling, design, and analysis with the Institute for Intelligent Systems Research and Innovation (IISRI), Deakin University. His research interests include mechatronics, component and systems analysis, design optimization for manufacture, and advanced manufacturing techniques.

NAVID MOHAJER received the B.Eng. degree in mechanical engineering, in 2009, the M.Sc. degree in mechatronics engineering, in 2012, and the Ph.D. degree in mechanical engineering and vehicle dynamics from Deakin University, Australia, in 2017. He is currently a Senior Research Fellow with the Institute for Intelligent Systems Research and Innovation (IISRI), Deakin University. He has been involved in several projects and has published several papers in high reputation journals and IEEE conferences. His research interests include mechanical design and analysis of complex systems, multibody systems (kinematics and dynamics), sensing, control, and actuation of autonomous systems.

DARIUS NAHAVANDI (Member, IEEE) received the Ph.D. degree from Deakin University, in 2018. He is currently a Research Fellow in human factors modeling and simulation with the Institute for Intelligent Systems Research and Innovation (IISRI), Deakin University. His research interests include human physiological data analysis, autonomous systems, and assistive exoskeleton systems.

PARHAM MOHSENZADEH KEBRIA (Member, IEEE) received the Ph.D. degree in information technology from Deakin University, Australia, in 2019. He is currently a Data Scientist and a Research Fellow in AI and robotics with the Institute for Intelligent Systems Research and Innovation (IISRI), Deakin University. His research interests include AI, medical robotics, and autonomous systems. He received the Alfred Deakin Postdoctoral Research Fellowship from IISRI, Deakin University, from 2020 to 2022.

SHADY MOHAMED received the Ph.D. degree from Deakin University, Australia, in 2009. He is currently an Associate Professor in signals and systems with the Institute for Intelligent Systems Research and Innovation (IISRI), Deakin University. His research interests include signal processing, human physiological data analysis, autonomous systems, and motion simulation.